

Status update on the MARA-LEB facility

Philippos Papadakis

LA³NET Workshop

25.10.2016

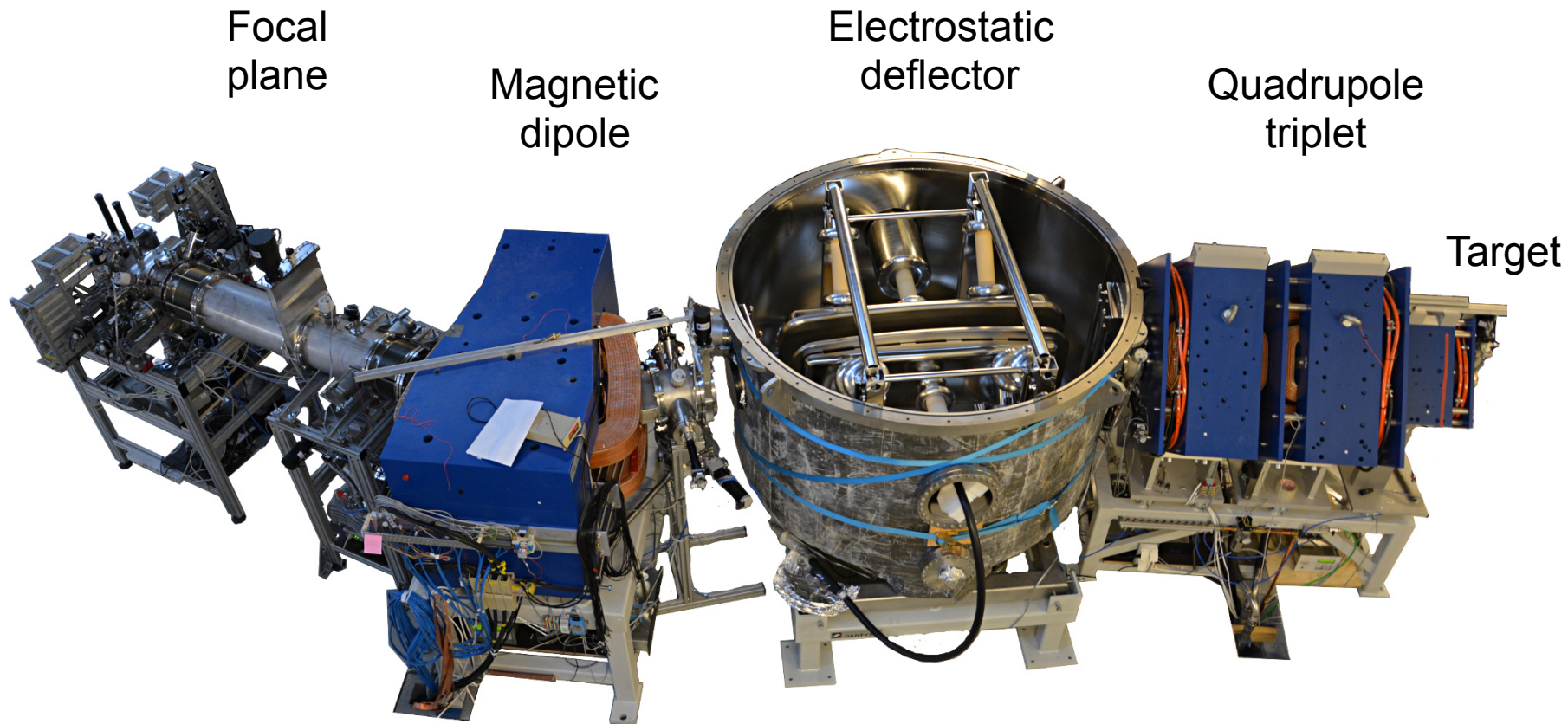
Outline

- The MARA vacuum-mode recoil-mass separator
 - Overview of separator
 - In-beam tests / first experiment
- The MARA-Low Energy Branch (MARA-LEB)
 - Scientific motivation
 - Components of MARA-LEB
 - Detector systems
 - Current status

The MARA vacuum-mode recoil-mass separator

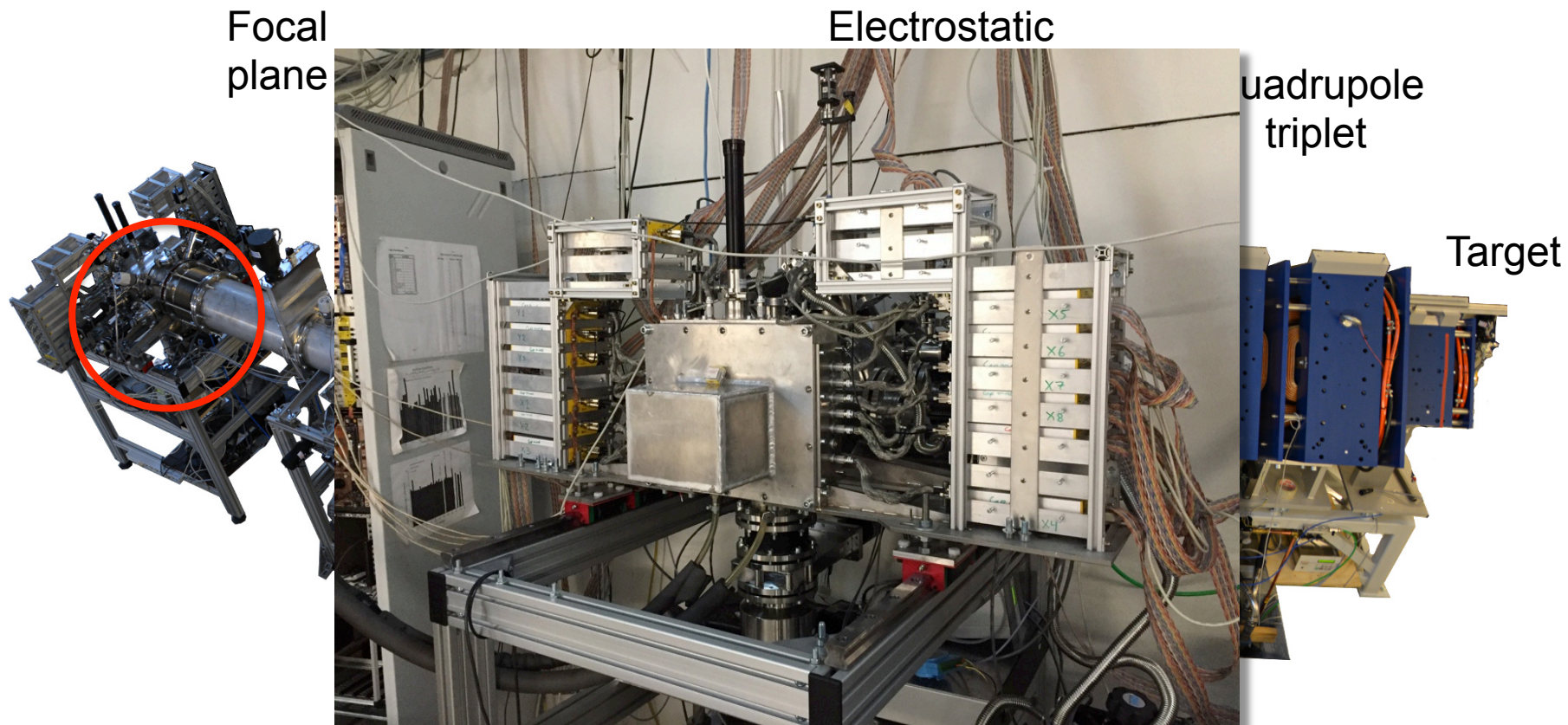
**Mass Analyzing Recoil Apparatus
Massa Analysoiva Rekyyli Aparatti**

The MARA vacuum-mode recoil-mass separator



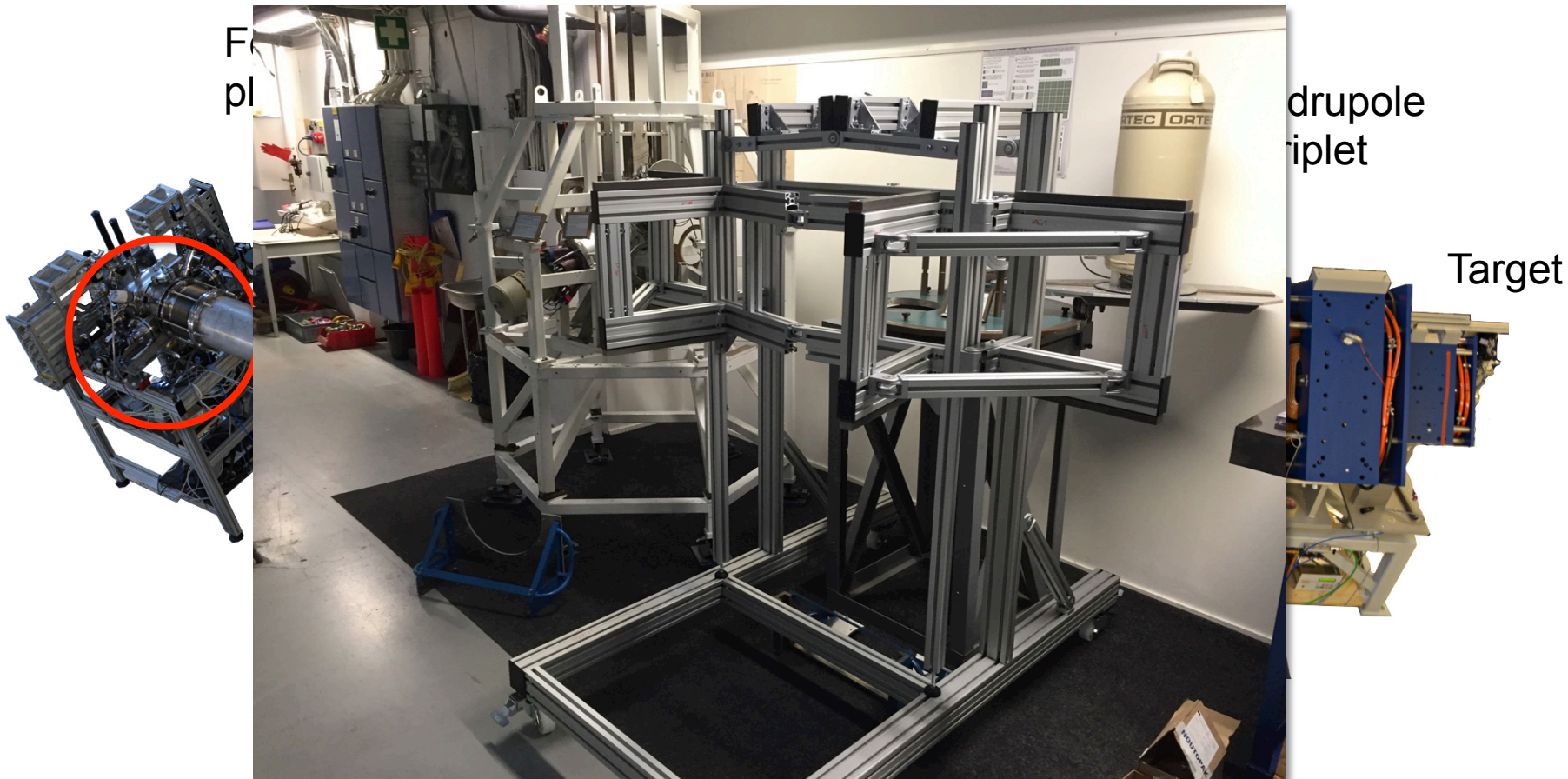
- 1st order mass resolving power: ~ 250
- Angular acceptance: 10msr

The MARA vacuum-mode recoil-mass separator



- DSSD (MICRON BB20)
- Punch-through detector
- Silicon box for escaped particles
- Germanium-detector array

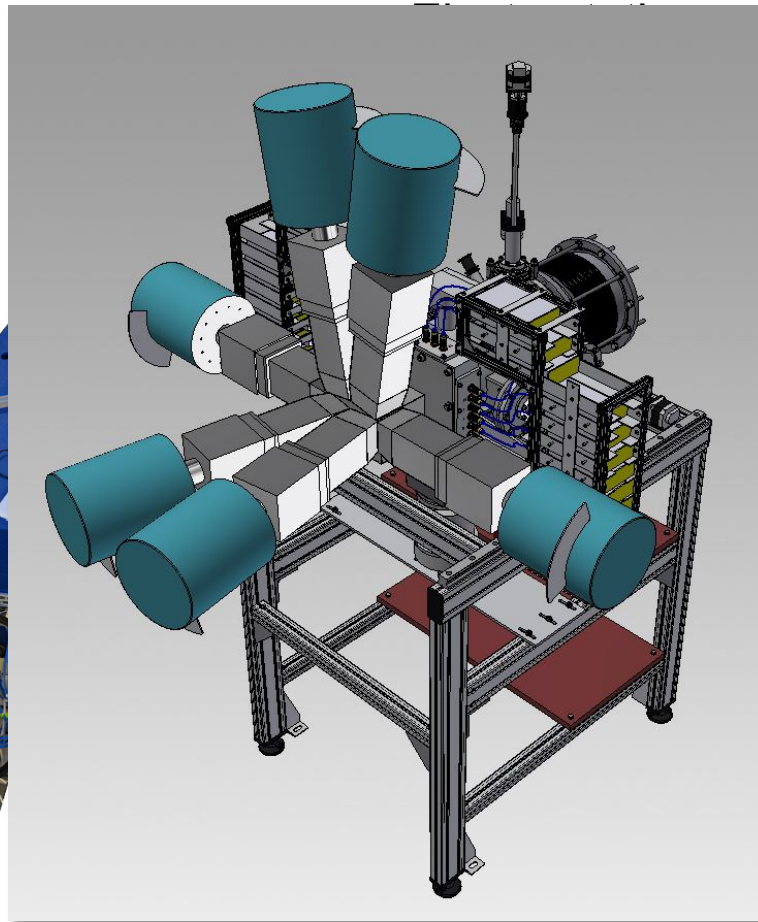
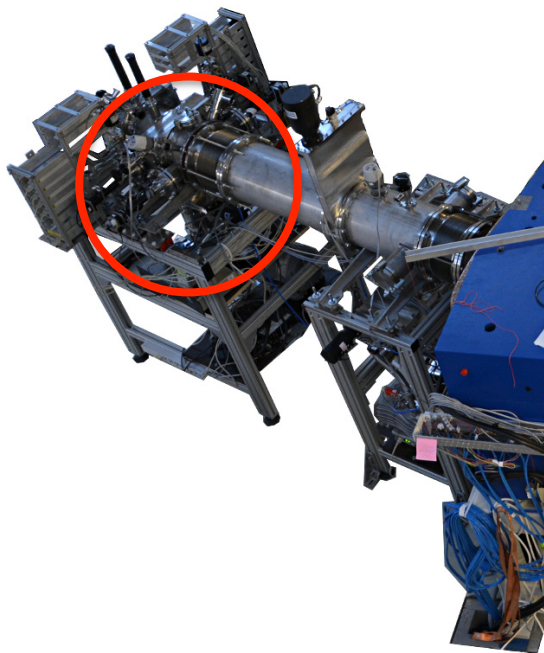
The MARA vacuum-mode recoil-mass separator



- DSSD (MICRON BB20)
- Punch-through detector
- Silicon box for escaped particles
- Germanium-detector array

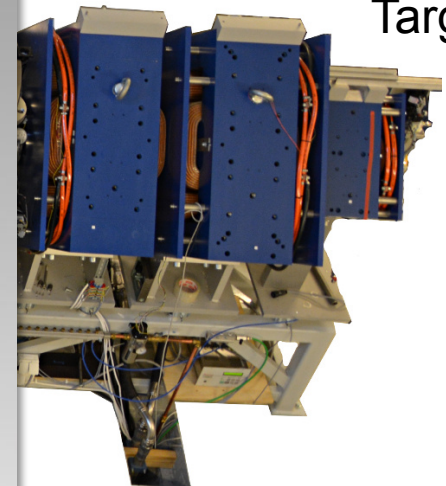
The MARA vacuum-mode recoil-mass separator

Focal
plane



Quadrupole
triplet

Target



- DSSD (MICRON BB20)
- Punch-through detector
- Silicon box for escaped particles
- Germanium-detector array

The MARA vacuum-mode recoil-mass separator



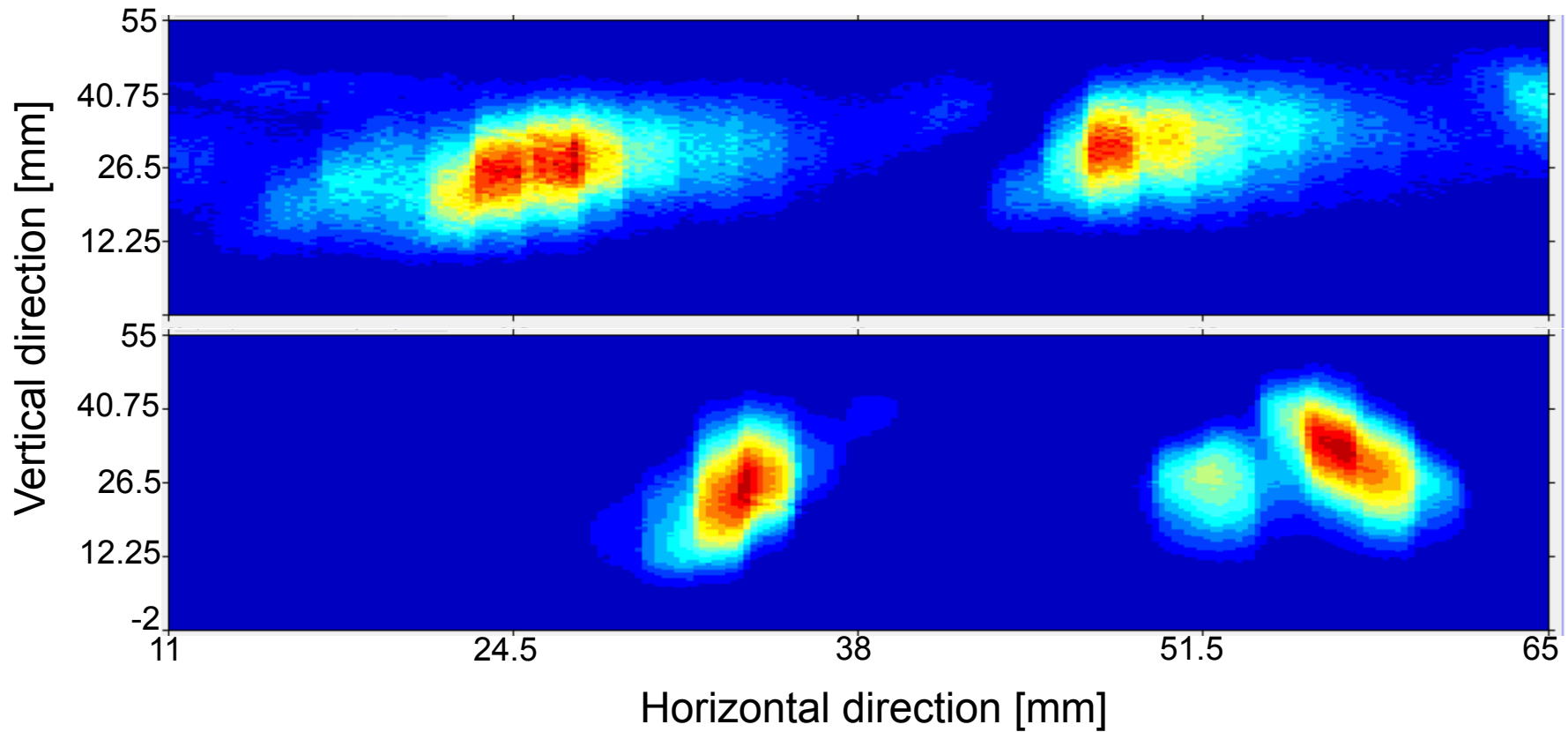
The MARA vacuum-mode recoil-mass separator



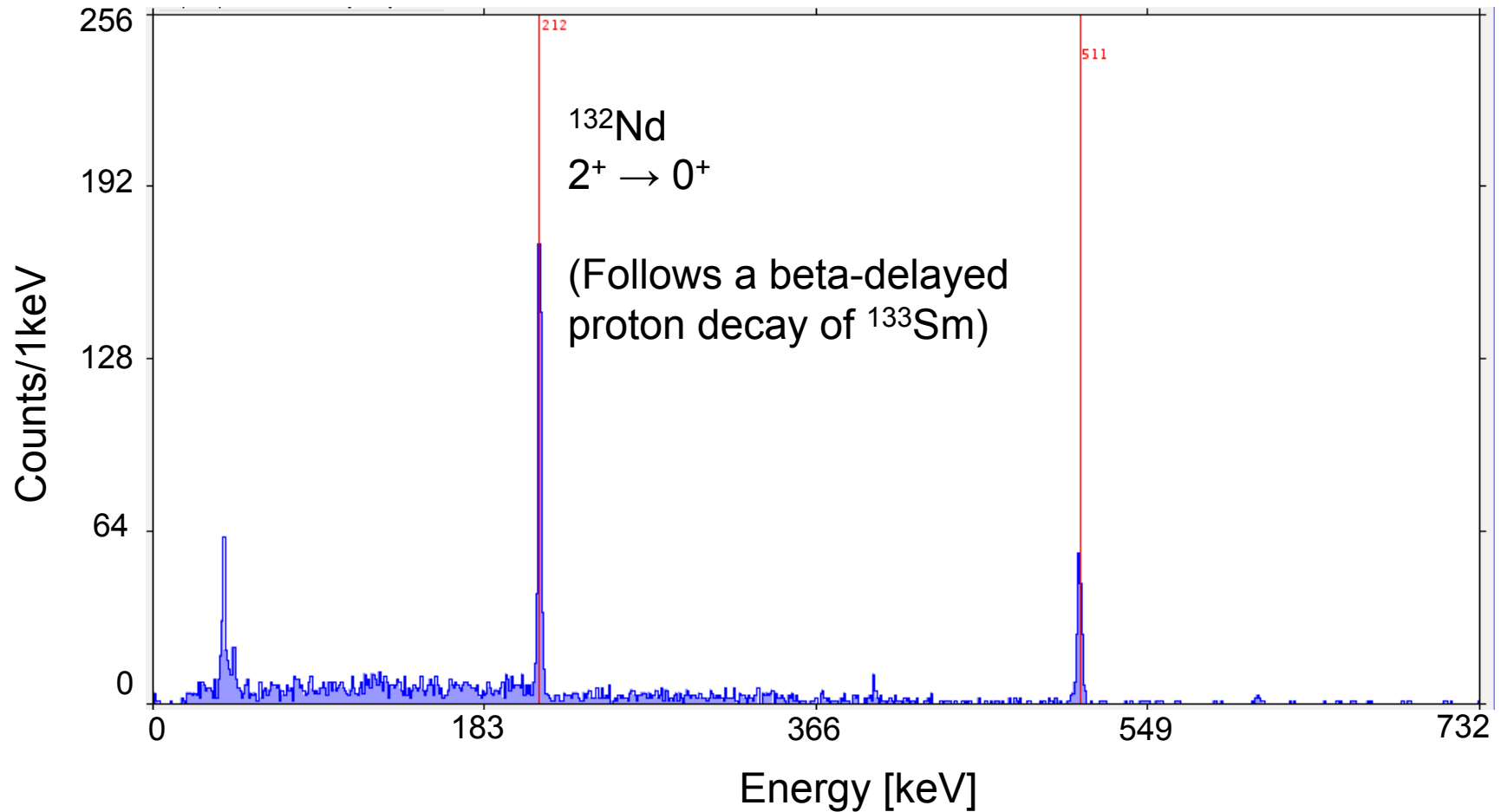
Commissioning runs (M01) this far

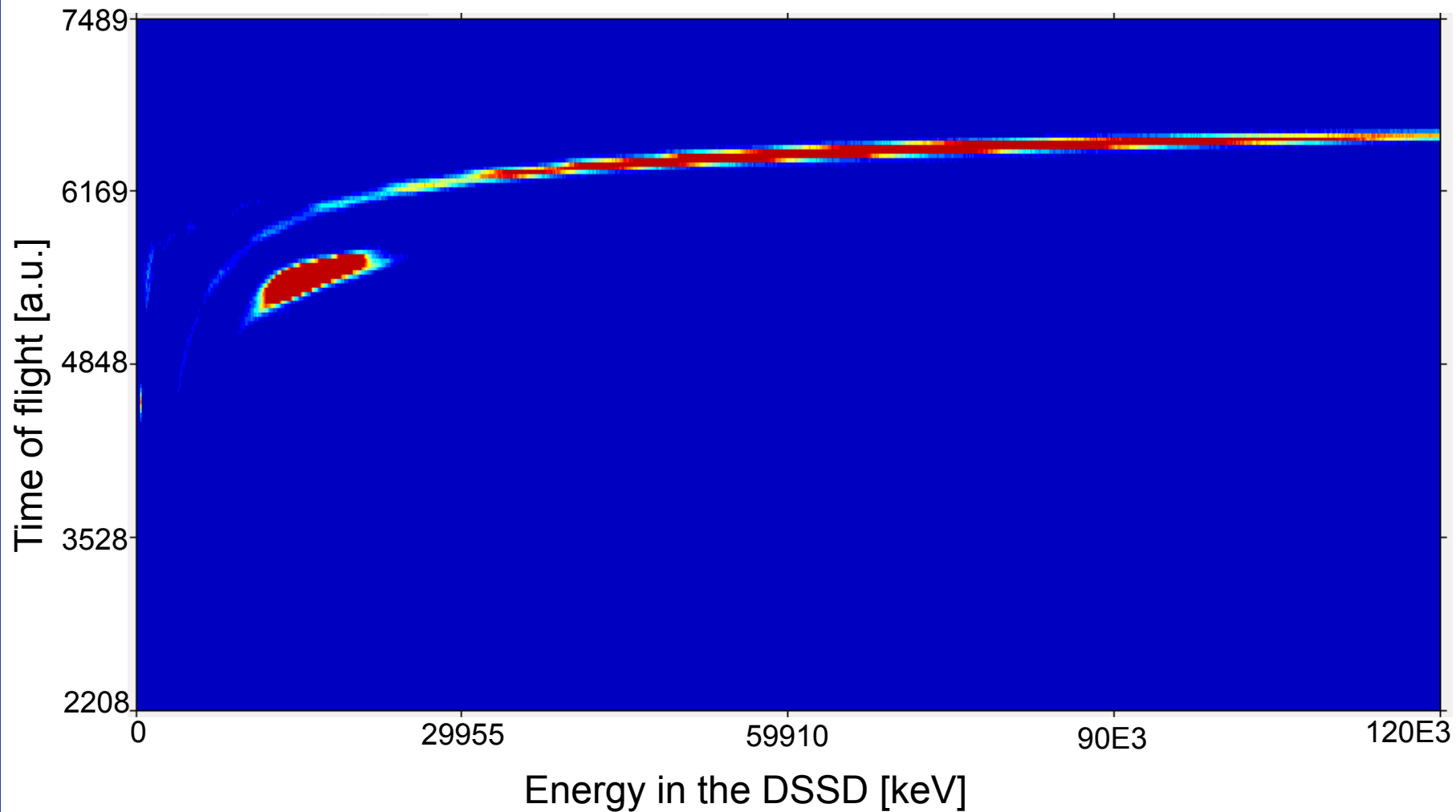
- Part 1: Slightly asymmetric
 - $^{78}\text{Kr} + ^{98}\text{Mo} \rightarrow ^{176}\text{Pt}^*$
- Part 2: Symmetric
 - $^{40}\text{Ar} + ^{45}\text{Sc} \rightarrow ^{85}\text{Nb}^*$
 - $^{40}\text{Ar} + ^{\text{nat}}\text{Ca} \rightarrow \sim^{80}\text{Sr}^*$
- Part 3: Inverse kinematics
 - $^{78}\text{Kr} + ^{58}\text{Ni} \rightarrow ^{136}\text{Gd}^*$
 - 2 BGO crystals around the target for normalization,
 - 2 Clover germanium detectors at the focal plane,
 - Punch through detector behind the DSSD
- Part 4: Asymmetric
 - $^{40}\text{Ar} + ^{124}\text{Sn} \rightarrow ^{164}\text{Er}^*$
 - 2 single crystal germanium detectors around the target,
 - Punch through detector behind the DSSD

Part 3: $^{78}\text{Kr} + ^{58}\text{Ni} \rightarrow ^{136}\text{Gd}^*$

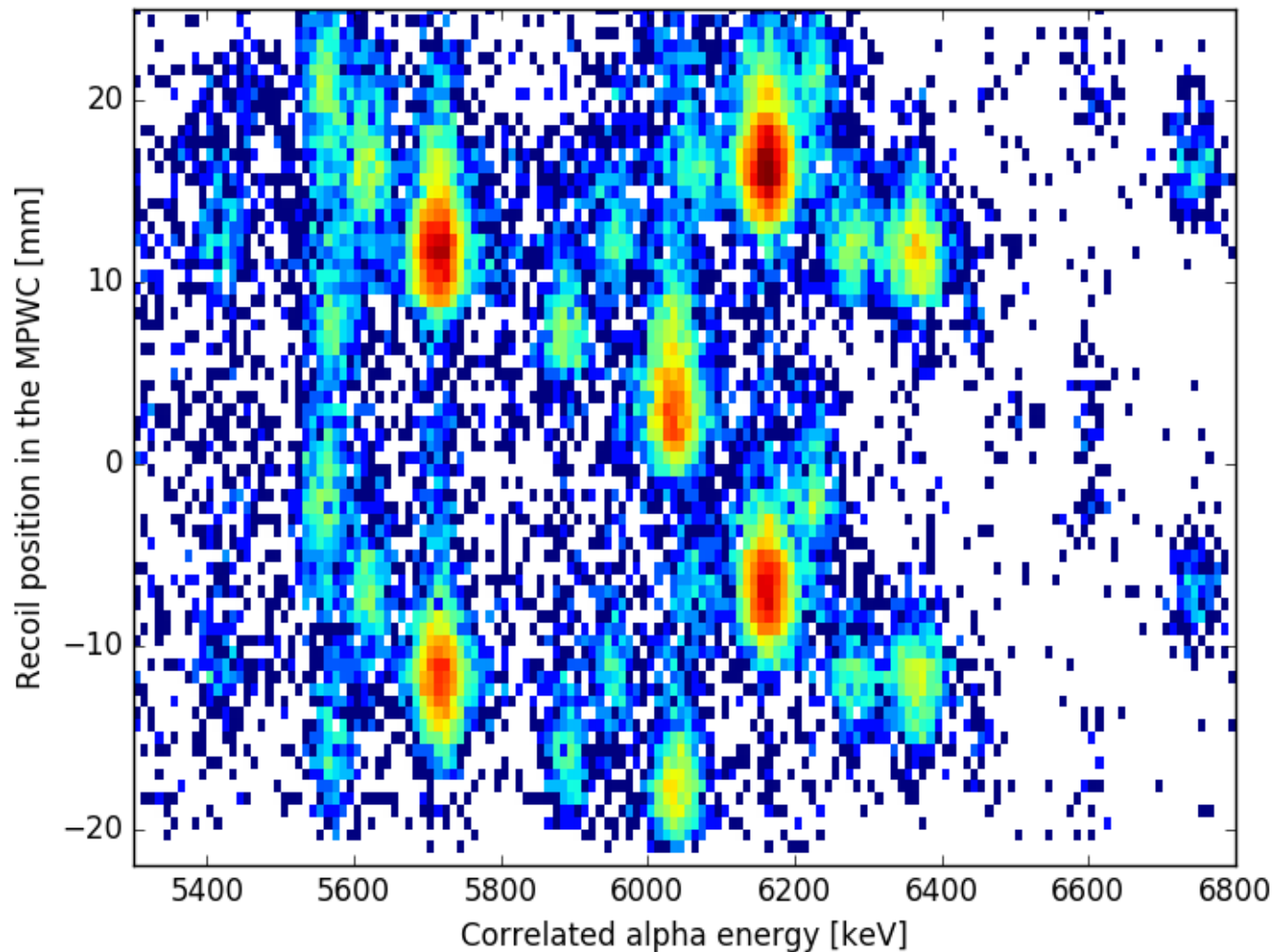


Part 3: $^{78}\text{Kr} + ^{58}\text{Ni} \rightarrow ^{136}\text{Gd}^*$

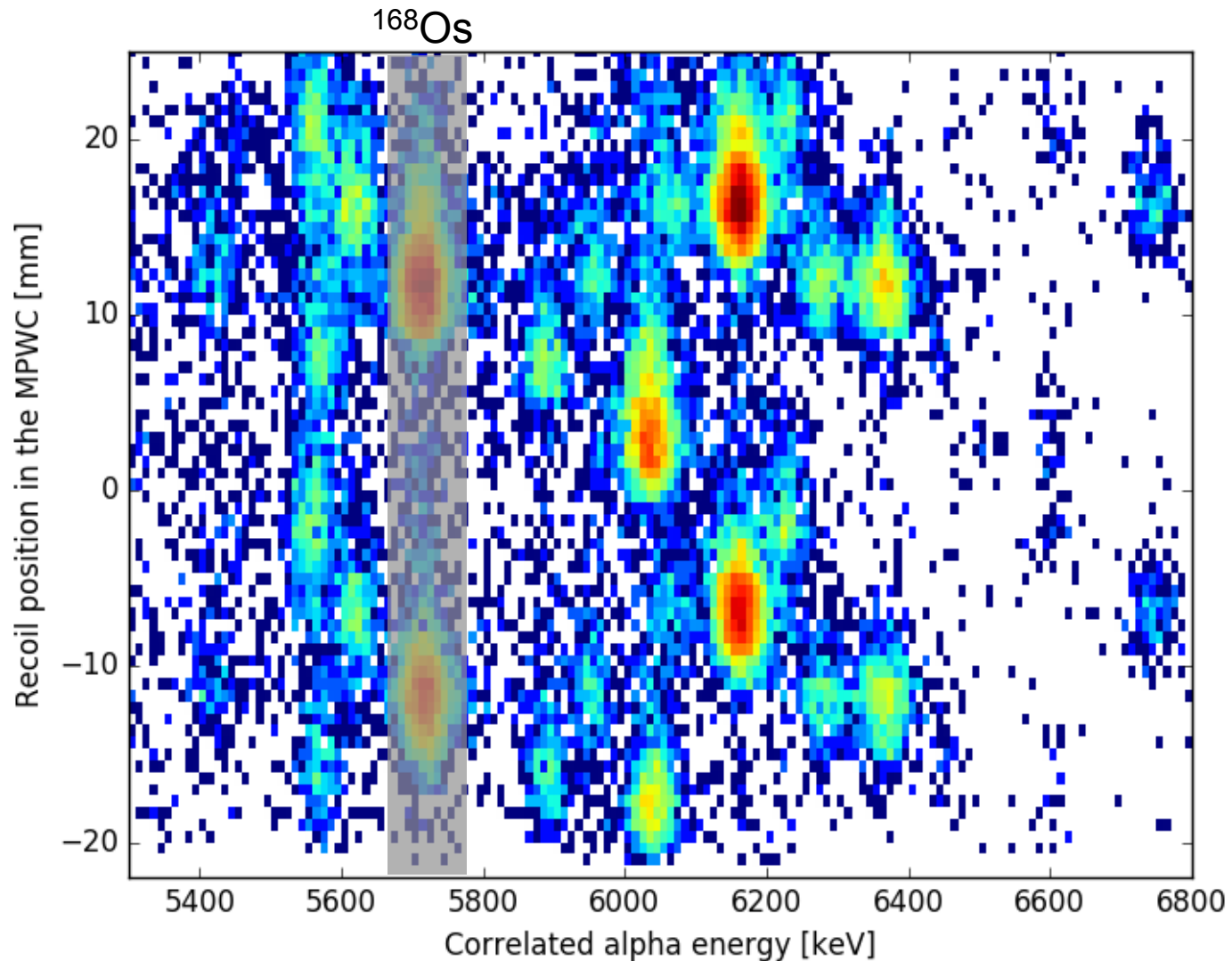


Part 4: $^{40}\text{Ar} + ^{124}\text{Sn} \rightarrow ^{164}\text{Er}^*$ 

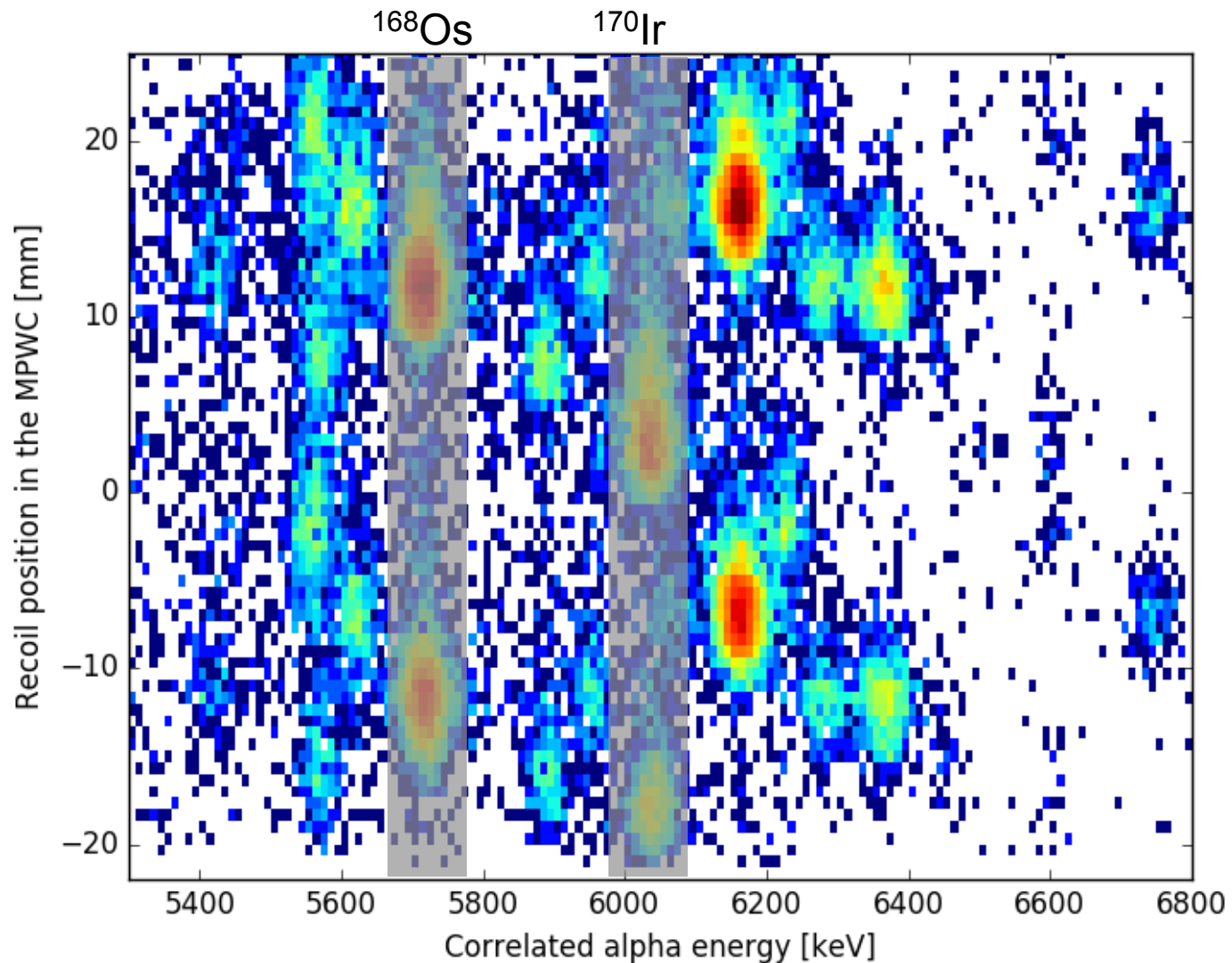
1st experiment: $^{78}\text{Kr} + ^{96}\text{Ru} \rightarrow ^{174}\text{Hg}^* \rightarrow ^{169}\text{Au}$



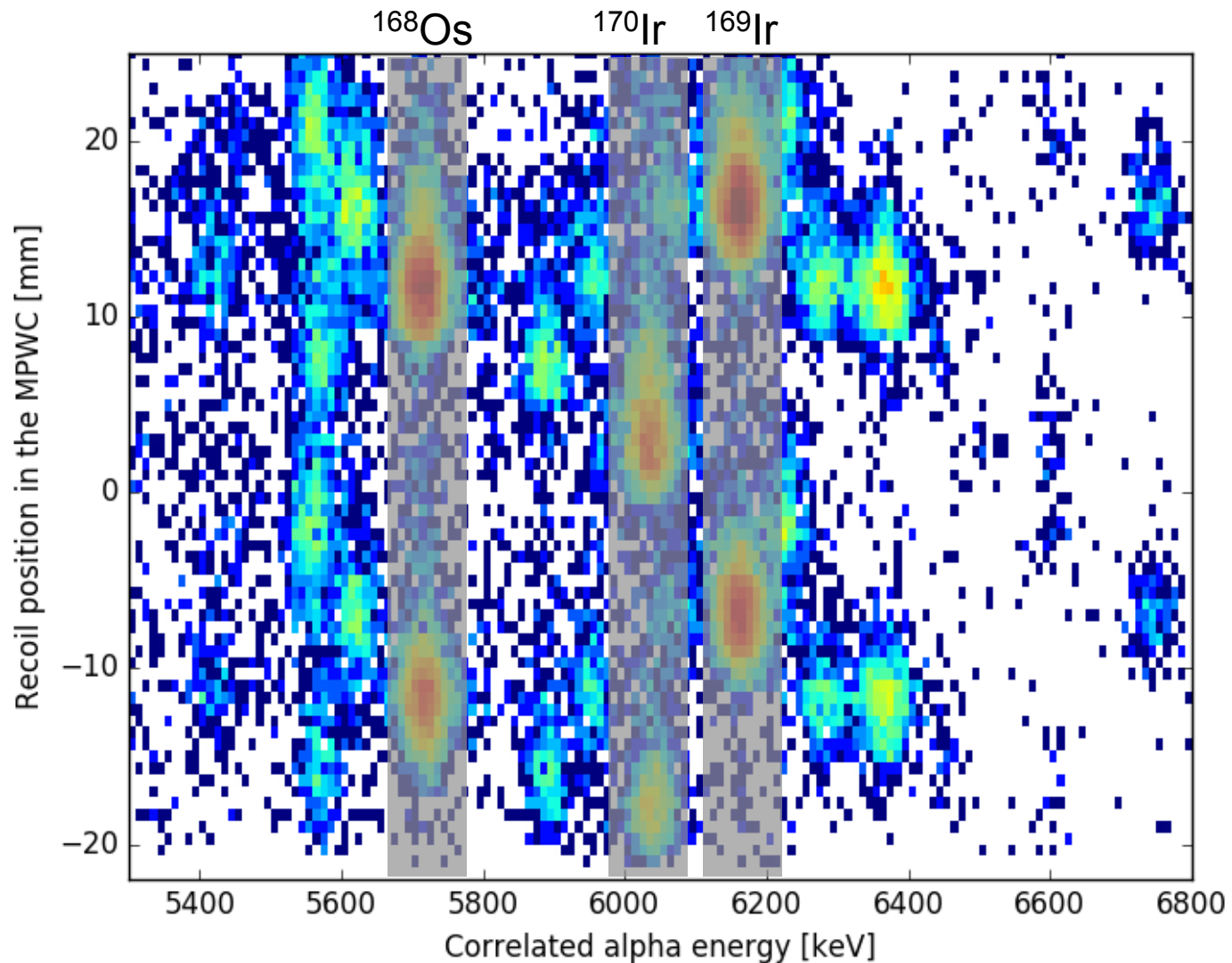
1st experiment: $^{78}\text{Kr} + ^{96}\text{Ru} \rightarrow ^{174}\text{Hg}^* \rightarrow ^{169}\text{Au}$



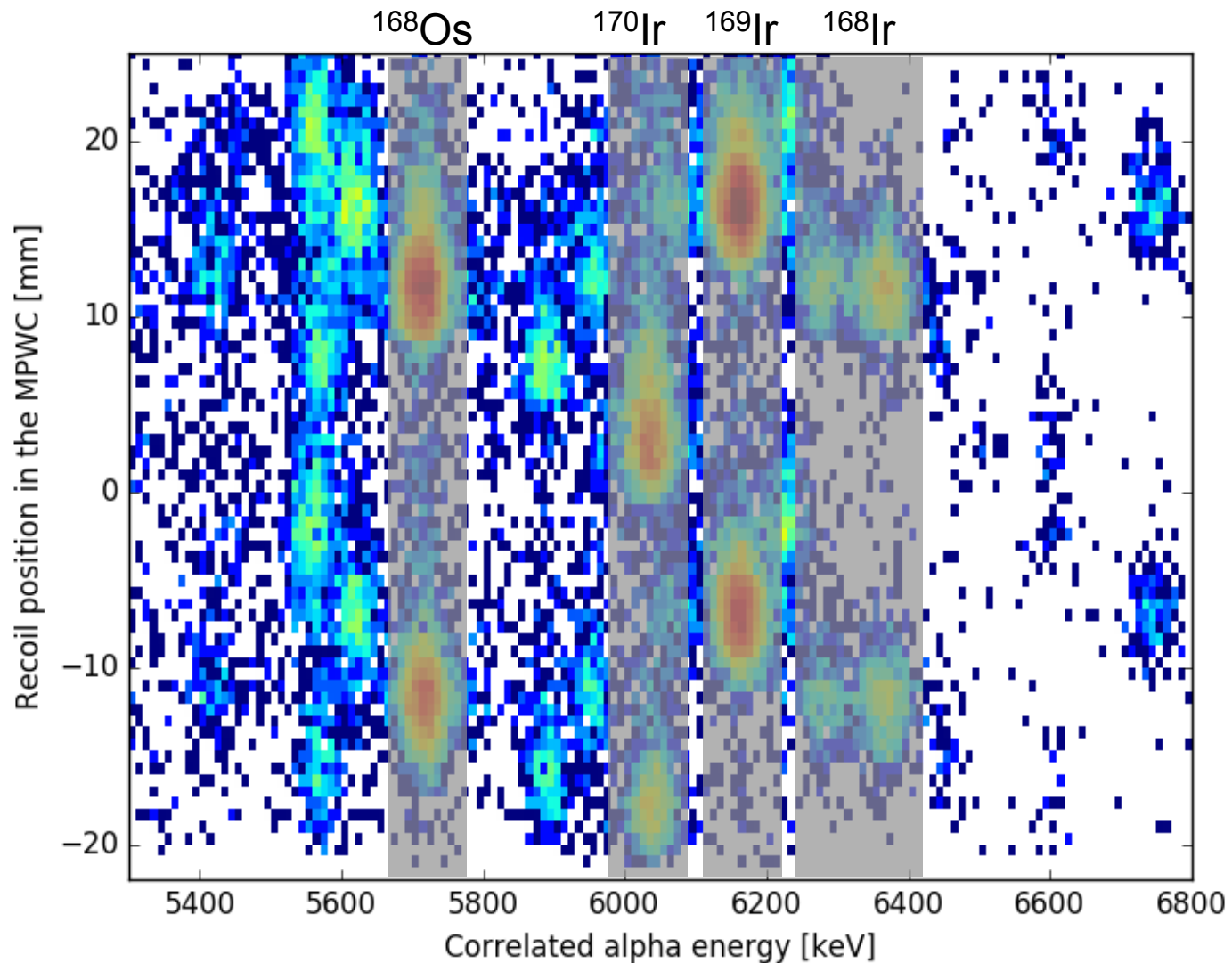
1st experiment: $^{78}\text{Kr} + ^{96}\text{Ru} \rightarrow ^{174}\text{Hg}^* \rightarrow ^{169}\text{Au}$



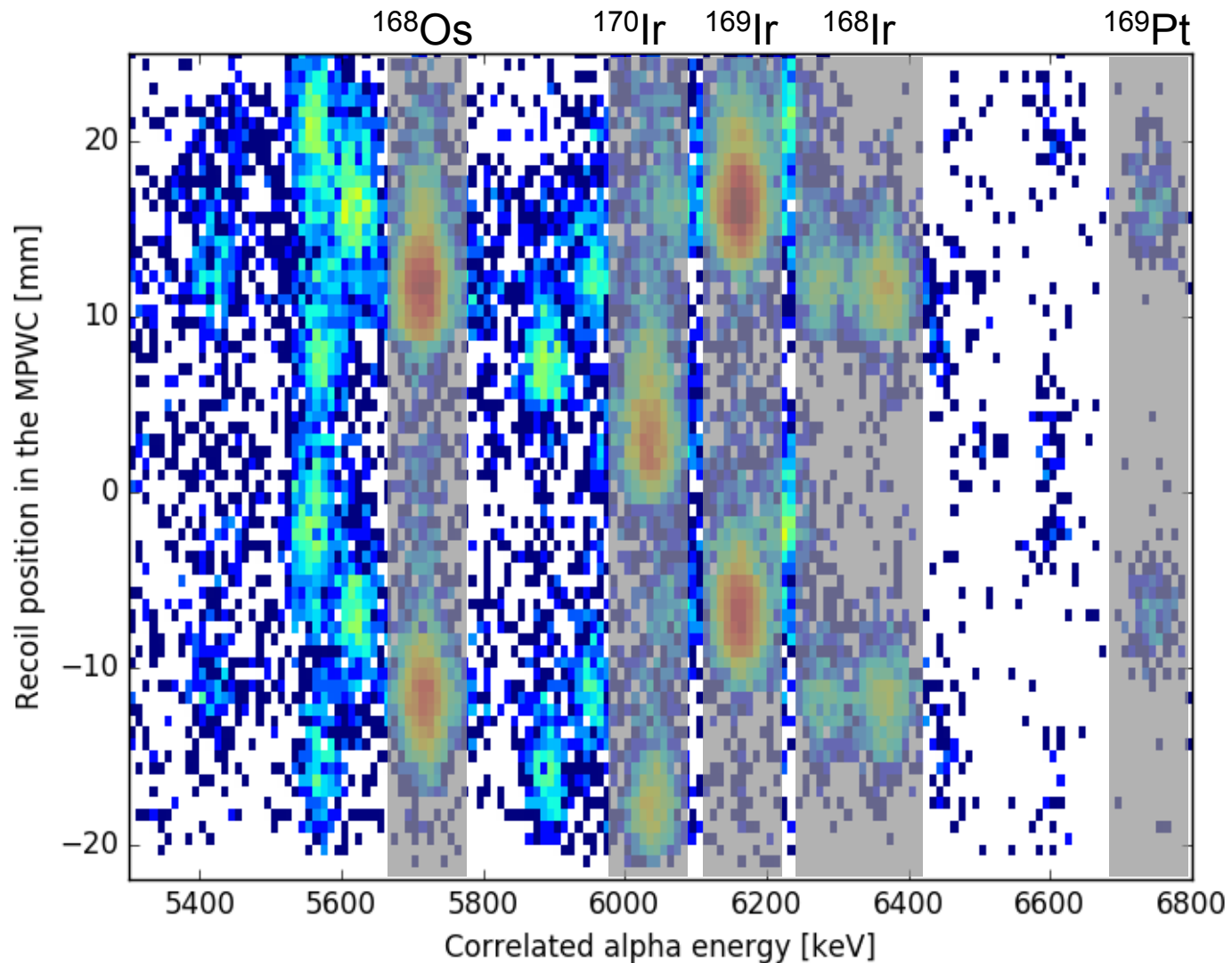
1st experiment: $^{78}\text{Kr} + ^{96}\text{Ru} \rightarrow ^{174}\text{Hg}^* \rightarrow ^{169}\text{Au}$



1st experiment: $^{78}\text{Kr} + ^{96}\text{Ru} \rightarrow ^{174}\text{Hg}^* \rightarrow ^{169}\text{Au}$

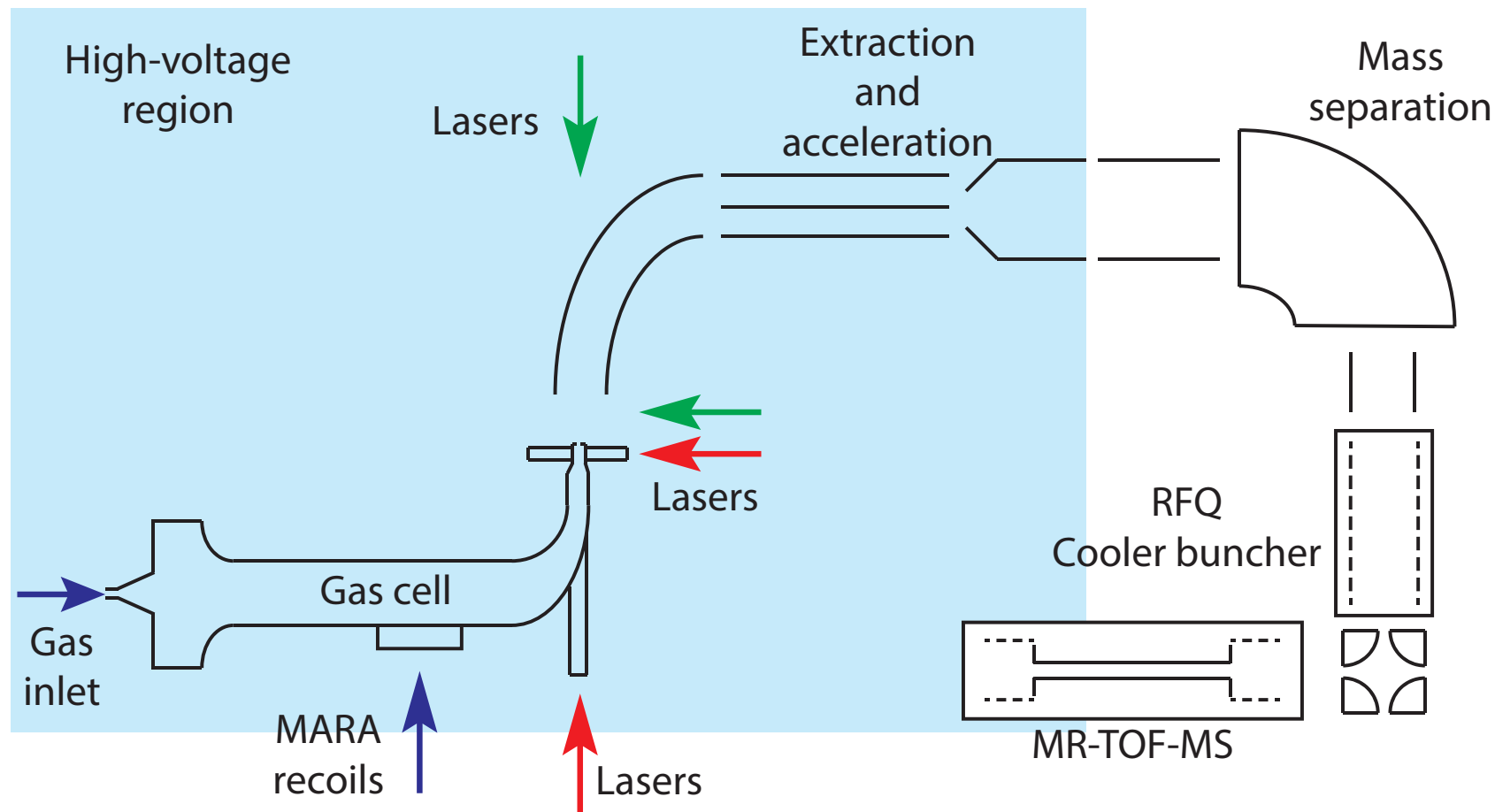


1st experiment: $^{78}\text{Kr} + ^{96}\text{Ru} \rightarrow ^{174}\text{Hg}^* \rightarrow ^{169}\text{Au}$



The MARA Low-Energy Branch

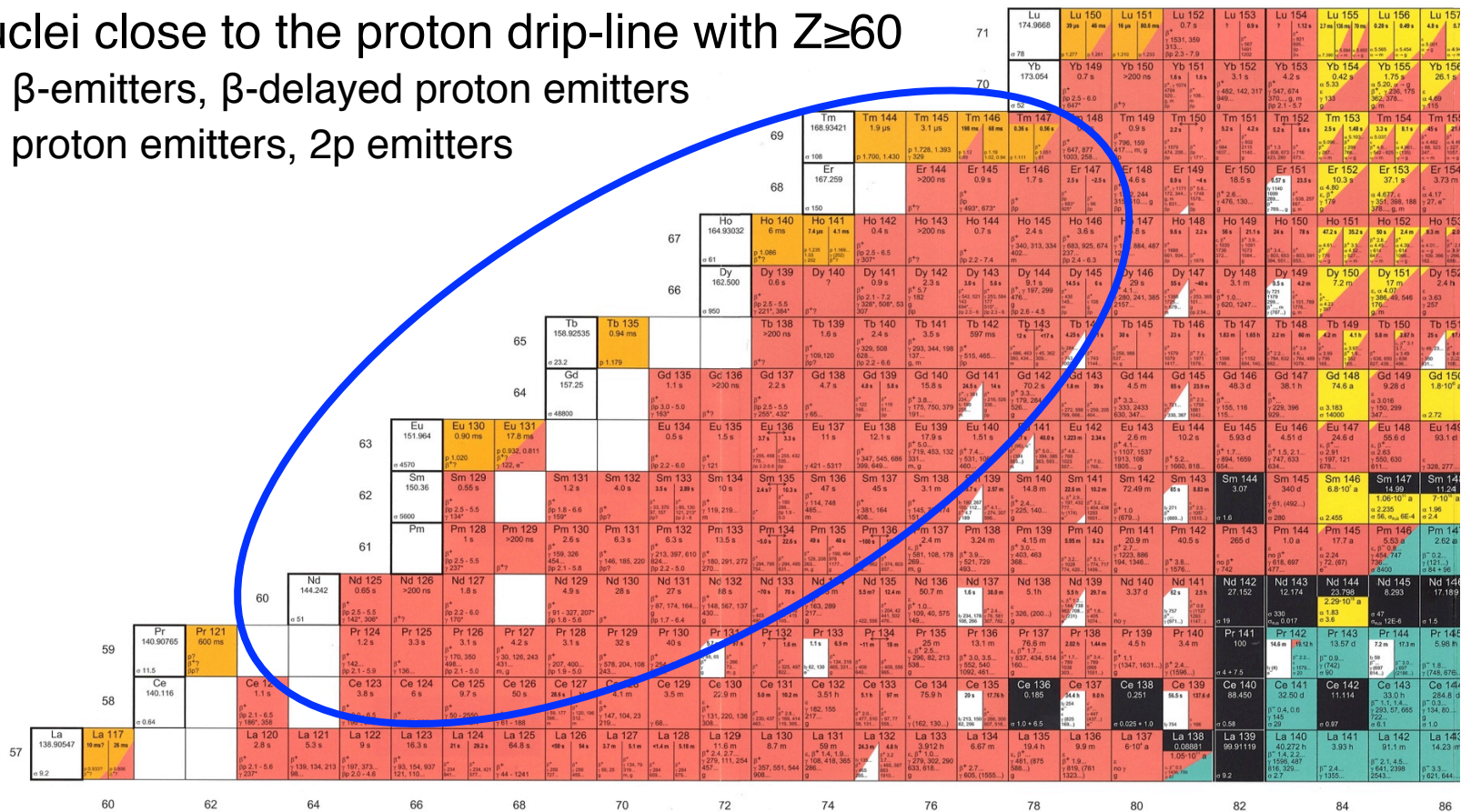
The concept of MARA-LEB



Motivation – A few examples

Nuclei close to the proton drip-line with $Z \geq 60$

- β -emitters, β -delayed proton emitters
- proton emitters, 2p emitters



Motivation – A few examples

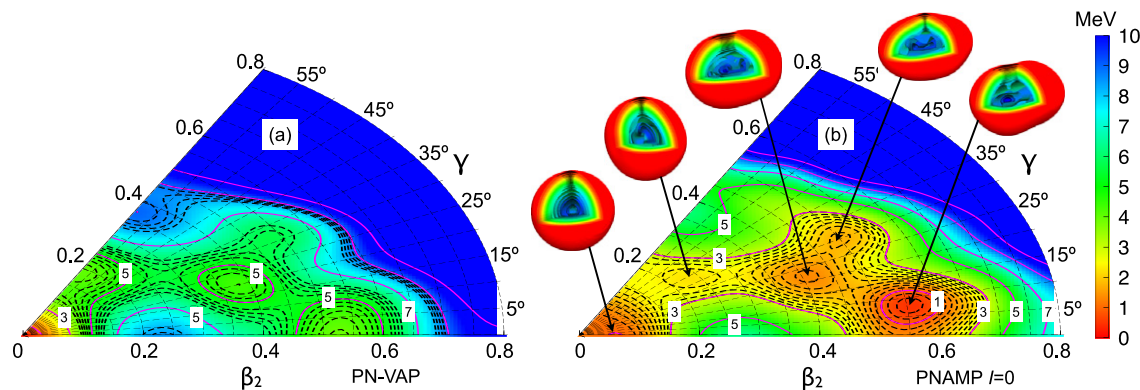
The image displays a comprehensive periodic table of elements, color-coded by groups. The table includes element symbols, atomic numbers, and names. It is organized into rows and columns, with the f-block elements (lanthanides and actinides) placed below the main body. The color-coding highlights various groups, such as the s-block (blue), p-block (various colors), d-block (orange), and f-block (yellow).

Data from :P. Campbell, I.D. Moore and M.R. Pearson, Progress in PNP **86**, 127 (2016)

Motivation – A few examples

^{80}Zr

- Highly deformed
- Theoretical predictions indicate coexistence of 5 shapes
- Waiting point of astrophysical rp-process

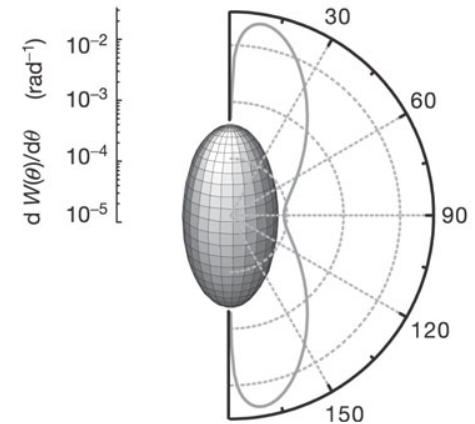


PN-VAP: Particle number symmetry restored
 PNAMP: Rotational symmetry also restored

Motivation – A few examples

$^{94}\text{Ag } 21^+$ Isomer

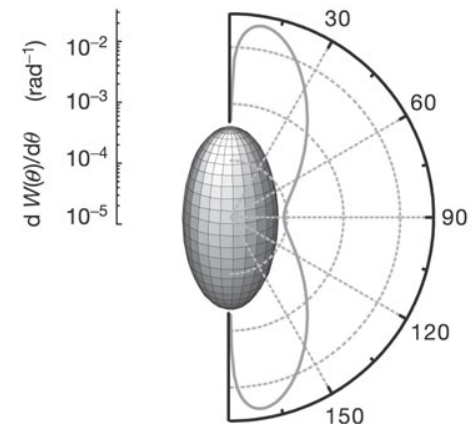
- I. Mukha *et al.*, Nature **439** (2006) 298
 - 1st nucleus to exhibit 1p and 2p radioactivity
 - Very large prolate deformation



Motivation – A few examples

$^{94}\text{Ag } 21^+$ Isomer

- I. Mukha *et al.*, Nature **439** (2006) 298
 - 1st nucleus to exhibit 1p and 2p radioactivity
 - Very large prolate deformation



- O. L. Pechenaya *et al.*, Phys. Rev. C **76** (2007) 011304(R)
 - No indication of 2p decay to ^{92}Rh
- J. Cerny *et al.*, Phys. Rev. Lett. **103** (2009) 152502
 - Confirmation of 1, 1p decay branch
 - No sign of the 2p decay
- A. Kankainen *et al.*, Phys. Rev. Lett. **101** (2008) 142503
 - Measurement of ^{92}Rh , ^{94}Pd mass with JYFLTRAP at IGISOL
 - Contradicting masses for $^{94}\text{Ag } 21^+$ isomer

Motivation – A few examples

Medical applications

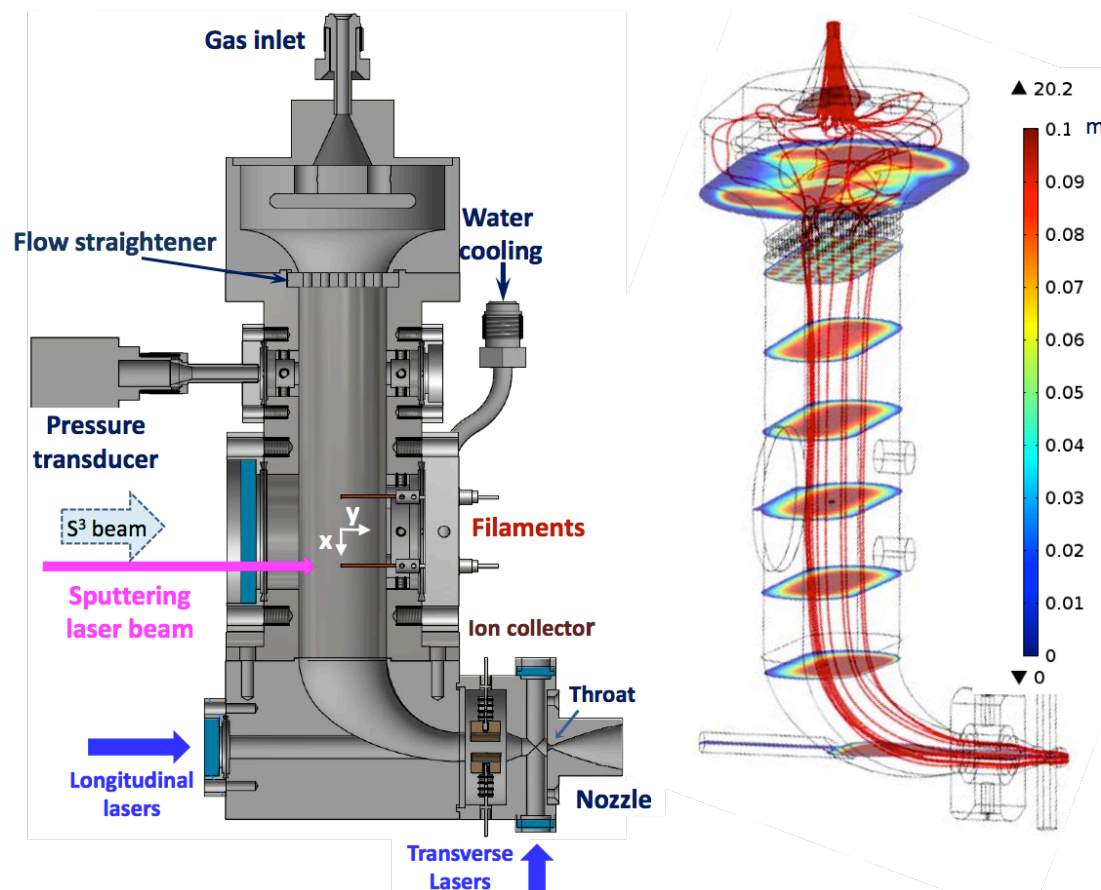
- Development of laser ionisation schemes
- Comparison of ionisation efficiencies

The image shows a portion of the periodic table, specifically the lanthanide and actinide series. The elements are arranged in rows and columns, with their atomic numbers, chemical symbols, and names listed. Several elements are circled in purple, and red diagonal lines are drawn across the table, likely indicating specific elements of interest for the research mentioned in the text.

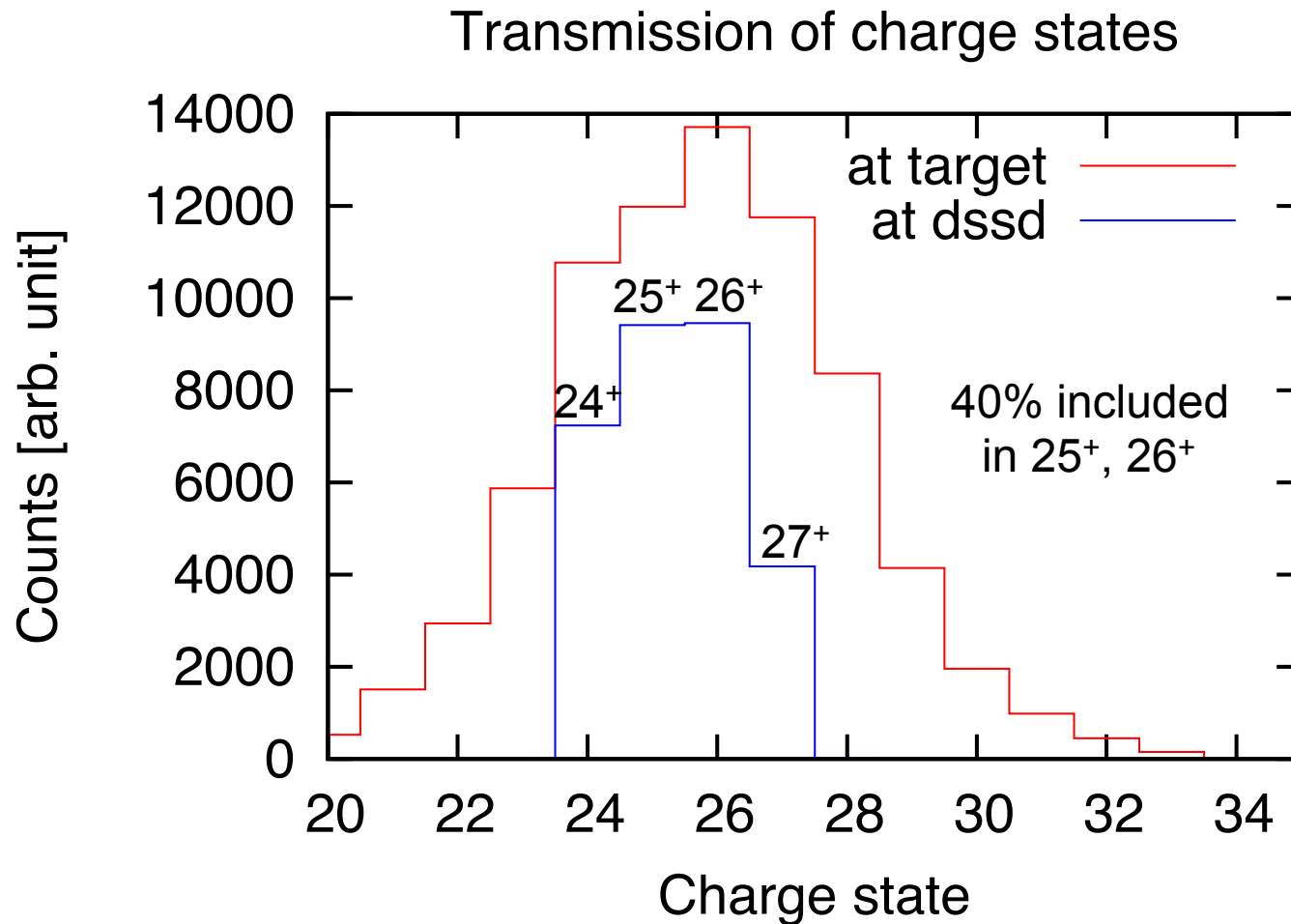
Ho 147 5.8 s β^+ 189, 884, 487 1264... m, g	Ho 148 9.6 s 2.2 s β^+ 1688 861, 504, 1078 g	Ho 149 21.1 s 24 s β^+ 1035 1736 372 g	Ho 150 78 s 24 s β^+ 3.4... 803, 591 394, 551 g	Ho 151 47.2 s 35.2 s β^+ 4.61... 803, 591 394, 551 g	Ho 152 50 s 2.4 m β^+ 2.8... 1614 1086 g	Ho 153 9.3 m 2.0 m β^+ 4.01... 1086, 366 296, 637 162 g	Ho 154 3.3 m 11.8 m β^+ 3.53... 335, 412 873 g	Ho 155 18 m 3.8 m β^+ 1.8... 240, 136... g	Ho 156 7.8 m 5.5 s 58 m β^+ 3.6... 159 38 g	Ho 157 12.6 m 21 m 27 m 11 m β^+ 1.2, 1.5... 280, 341, 193 87... g	Ho 158 21 m 27 m 11 m β^+ 1.3... 118 100 g	Ho 159 8.3 s 33 m 3 s 5.0 h 26 m 6 s 2.5 h β^+ 1.1... 121, 132 310, 253 g	Ho 160 3 s 5.0 h 26 m 6 s 2.5 h β^+ 1.1... 121, 132 310, 253 g	Ho 161 6 s 2.5 h β^+ 1.1... 121, 132 310, 253 g	Ho 162 68 m 15 m 1.1 s 4570 a 37 m 29 m β^+ 1.0... 121, 132 310, 253 g	Ho 163 1.1 s 4570 a 37 m 29 m β^+ 1.0... 121, 132 310, 253 g	Ho 164 37 m 29 m β^+ 1.0... 121, 132 310, 253 g
Dy 146 29 s β^+ 4.1... 280, 241, 385 2157... g	Dy 147 55 s 40 s β^+ 1.0... 253, 305 1736 g	Dy 148 3.1 m 4.2 m β^+ 1.0... 253, 305 1736 g	Dy 149 4.2 m 17 m β^+ 1.0... 253, 305 1736 g	Dy 150 7.2 m 17 m β^+ 1.0... 253, 305 1736 g	Dy 151 17 m 4 h β^+ 1.0... 253, 305 1736 g	Dy 152 4 h 17 m β^+ 1.0... 253, 305 1736 g	Dy 153 6.29 h 17 m β^+ 1.0... 253, 305 1736 g	Dy 154 3.0-10 ⁶ a 17 m β^+ 1.0... 253, 305 1736 g	Dy 155 3.0 h 17 m β^+ 1.0... 253, 305 1736 g	Dy 156 0.056 17 m β^+ 1.0... 253, 305 1736 g	Dy 157 8.1 h 17 m β^+ 1.0... 253, 305 1736 g	Dy 158 0.095 17 m β^+ 1.0... 253, 305 1736 g	Dy 159 144.4 d 17 m β^+ 1.0... 253, 305 1736 g	Dy 160 2.329 17 m β^+ 1.0... 253, 305 1736 g	Dy 161 3.889 17 m β^+ 1.0... 253, 305 1736 g	Dy 162 25.475 17 m β^+ 1.0... 253, 305 1736 g	Dy 163 24.896 17 m β^+ 1.0... 253, 305 1736 g
Tb 145 30 s 17 m β^+ 1.0... 253, 305 1736 g	Tb 146 1.83 m 1.65 h 17 m β^+ 1.0... 253, 305 1736 g	Tb 147 1.83 m 1.65 h 17 m β^+ 1.0... 253, 305 1736 g	Tb 148 2.2 m 17 m β^+ 1.0... 253, 305 1736 g	Tb 149 4.1 h 17 m β^+ 1.0... 253, 305 1736 g	Tb 150 3.67 h 17 m β^+ 1.0... 253, 305 1736 g	Tb 151 25 s 17 m β^+ 1.0... 253, 305 1736 g	Tb 152 4.2 h 17.5 h 17 m β^+ 1.0... 253, 305 1736 g	Tb 153 2.34 d 17 m β^+ 1.0... 253, 305 1736 g	Tb 154 3.2 d 17 m β^+ 1.0... 253, 305 1736 g	Tb 155 32 d 17 m β^+ 1.0... 253, 305 1736 g	Tb 156 2.4 h 17 m β^+ 1.0... 253, 305 1736 g	Tb 157 99 a 17 m β^+ 1.0... 253, 305 1736 g	Tb 158 10.5 s 180 a 17 m β^+ 1.0... 253, 305 1736 g	Tb 159 100 17 m β^+ 1.0... 253, 305 1736 g	Tb 160 72.3 d 17 m β^+ 1.0... 253, 305 1736 g	Tb 161 90 d 17 m β^+ 1.0... 253, 305 1736 g	Tb 162 7.76 m 17 m β^+ 1.0... 253, 305 1736 g
Gd 144 4.5 m β^+ 3.3... 333, 2433 630, 347... g	Gd 145 23.9 m 48.3 d β^+ 2.3... 1788 115... g	Gd 146 48.3 d 17 m β^+ 2.3... 1788 115... g	Gd 147 38.1 h 17 m β^+ 2.3... 1788 115... g	Gd 148 74.6 a 17 m β^+ 2.3... 1788 115... g	Gd 149 28 d 17 m β^+ 2.3... 1788 115... g	Gd 150 1.8-10 ⁶ a 17 m β^+ 2.3... 1788 115... g	Gd 151 120 d 17 m β^+ 2.3... 1788 115... g	Gd 152 2.34 d 17 m β^+ 2.3... 1788 115... g	Gd 153 239.47 d 17 m β^+ 2.3... 1788 115... g	Gd 154 2.18 17 m β^+ 2.3... 1788 115... g	Gd 155 1.80 17 m β^+ 2.3... 1788 115... g	Gd 156 20.47 17 m β^+ 2.3... 1788 115... g	Gd 157 15.65 17 m β^+ 2.3... 1788 115... g	Gd 158 24.84 17 m β^+ 2.3... 1788 115... g	Gd 159 18.48 h 17 m β^+ 2.3... 1788 115... g	Gd 160 21.86 17 m β^+ 2.3... 1788 115... g	Gd 161 1.66 m 17 m β^+ 2.3... 1788 115... g
Eu 143 2.6 m β^+ 4.1... 1107, 1537 1913, 108 1805... g	Eu 144 10.2 s 5.93 d β^+ 5.2... 1660, 818... g	Eu 145 5.93 d 17 m β^+ 5.2... 1660, 818... g	Eu 146 4.51 d 17 m β^+ 5.2... 1660, 818... g	Eu 147 24.6 d 17 m β^+ 5.2... 1660, 818... g	Eu 148 55.6 d 17 m β^+ 5.2... 1660, 818... g	Eu 149 3.1 d 17 m β^+ 5.2... 1660, 818... g	Eu 150 12.8 h 36.9 a 17 m β^+ 5.2... 1660, 818... g	Eu 151 47.81 17 m β^+ 5.2... 1660, 818... g	Eu 152 19 m 17 m β^+ 5.2... 1660, 818... g	Eu 153 52.19 17 m β^+ 5.2... 1660, 818... g	Eu 154 46.0 m 17 m β^+ 5.2... 1660, 818... g	Eu 155 161 a 17 m β^+ 5.2... 1660, 818... g	Eu 156 15.2 d 17 m β^+ 5.2... 1660, 818... g	Eu 157 15.18 h 17 m β^+ 5.2... 1660, 818... g	Eu 158 46 m 17 m β^+ 5.2... 1660, 818... g	Eu 159 18.1 m 17 m β^+ 5.2... 1660, 818... g	Eu 160 42 s 17 m β^+ 5.2... 1660, 818... g

The gas cell

Designed by KU Leuven to be used for the rare element in-gas laser ion source (REGLIS) at S³, GANIL.



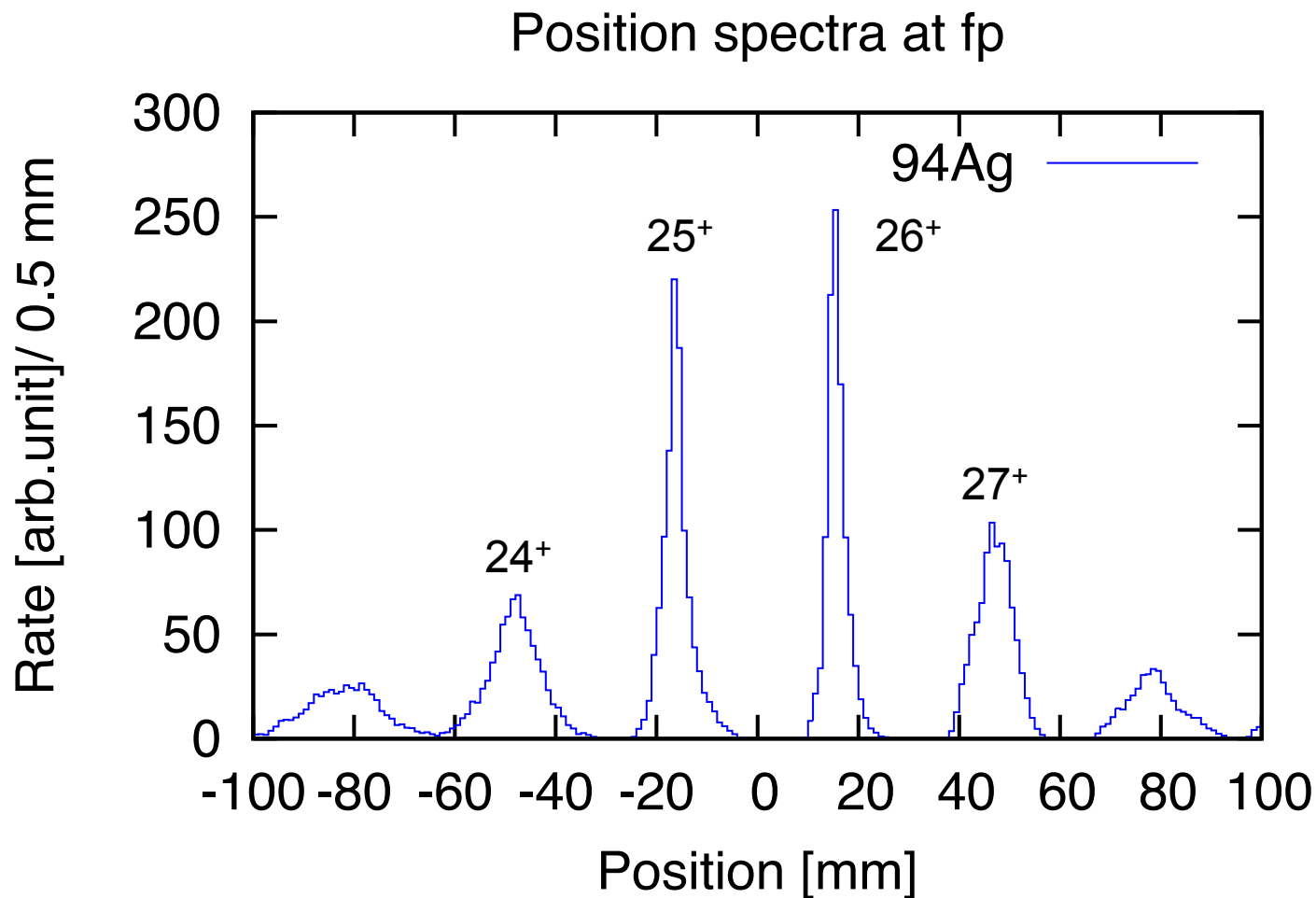
Recoil distributions at the focal plane



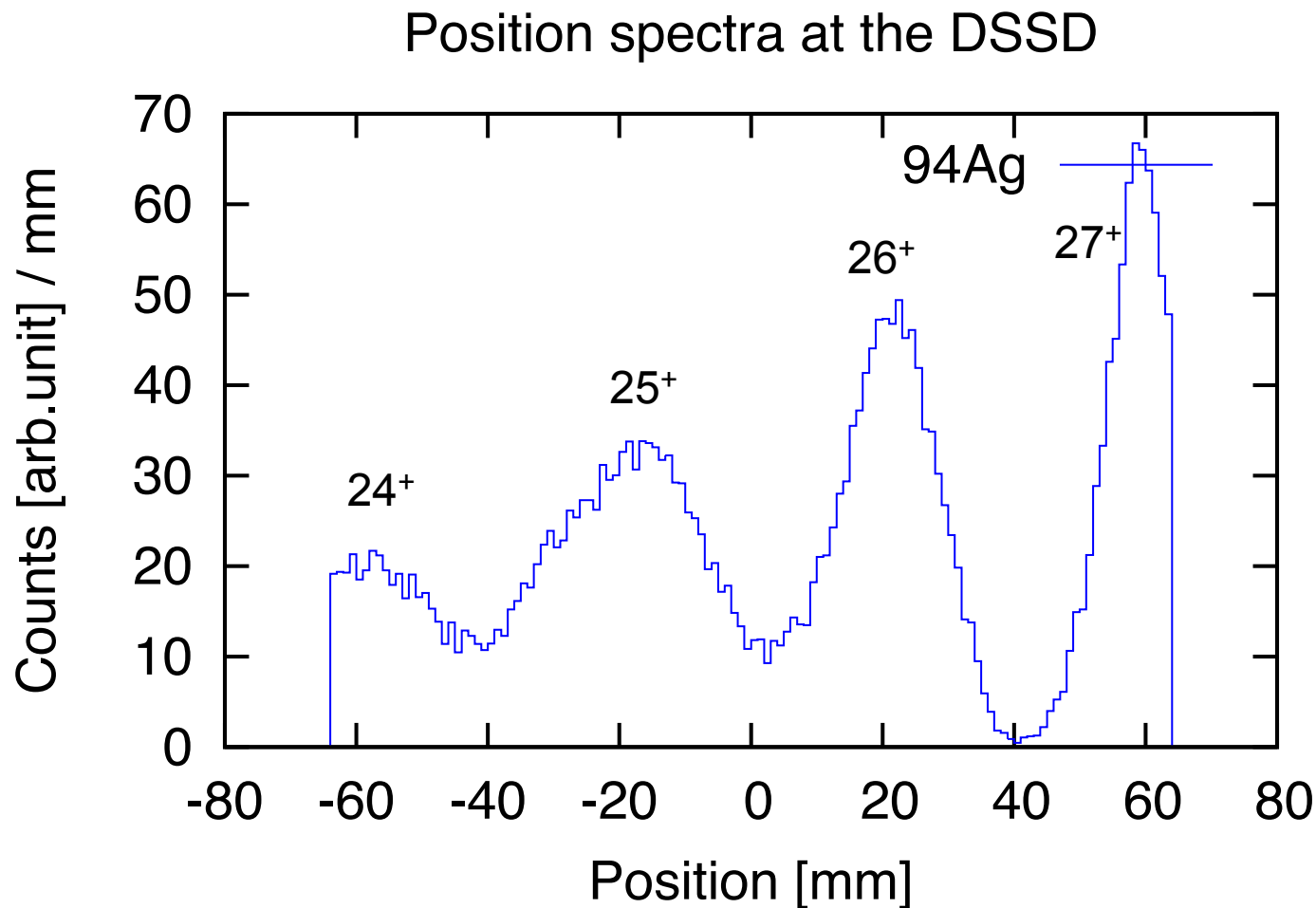
Production of ^{94}Ag

- $^{58}\text{Ni}(^{40}\text{Ca}, p3n)^{94}\text{Ag}$, 200pnA, 240MeV, $500\mu\text{g}/\text{cm}^2$
- ^{94}Ag cross section $\sim 500\text{n barn}$
- MARA transmission efficiency for the 2 most abundant charge states in inverse kinematics: $\varepsilon = 0.4 \times 0.8$
- ^{94}Ag at the MARA focal plane: ~ 1.5 ions/s
- Efficiency for resonance ionisation spectroscopy: $\sim 12\%$
 - 50% thermalisation, transport efficiency, 50% neutralisation, 50% in-gas-jet laser ionisation
 - Yield of ^{94}Ag : ~ 0.2 ions/s
- Efficiency to the MR-TOF-MS: $\sim 27\%$
 - 50% thermalisation, transport efficiency, 90% to the cooler and buncher, 60% efficiency through the buncher
 - Yield of ^{94}Ag : ~ 0.4 ions/s

Recoil distributions at the focal plane



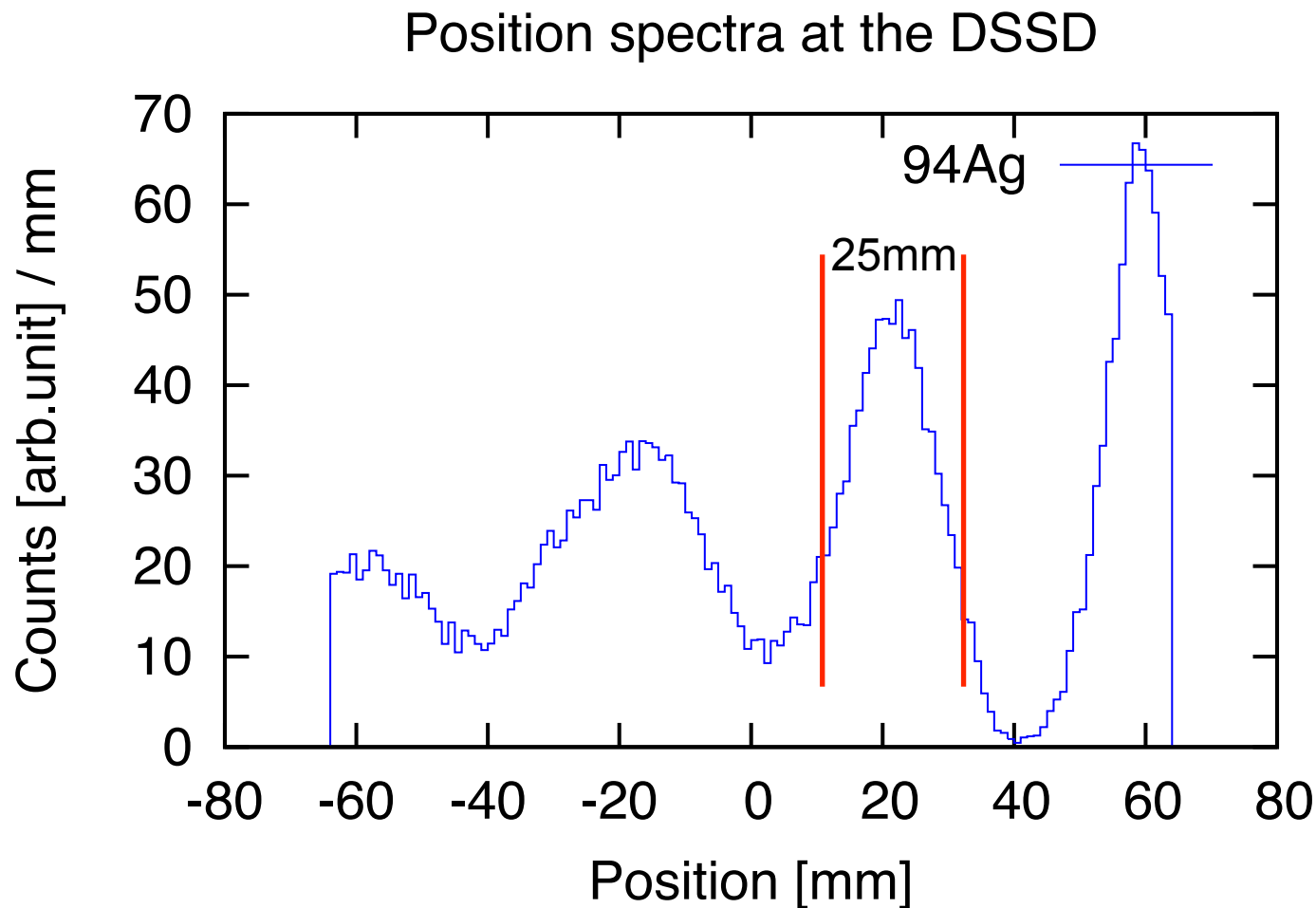
Recoil distributions at the focal plane



$^{58}\text{Ni}(^{40}\text{Ca}, p3n)^{94}\text{Ag}$ @ 192 MeV

Calculations by J. Sarén

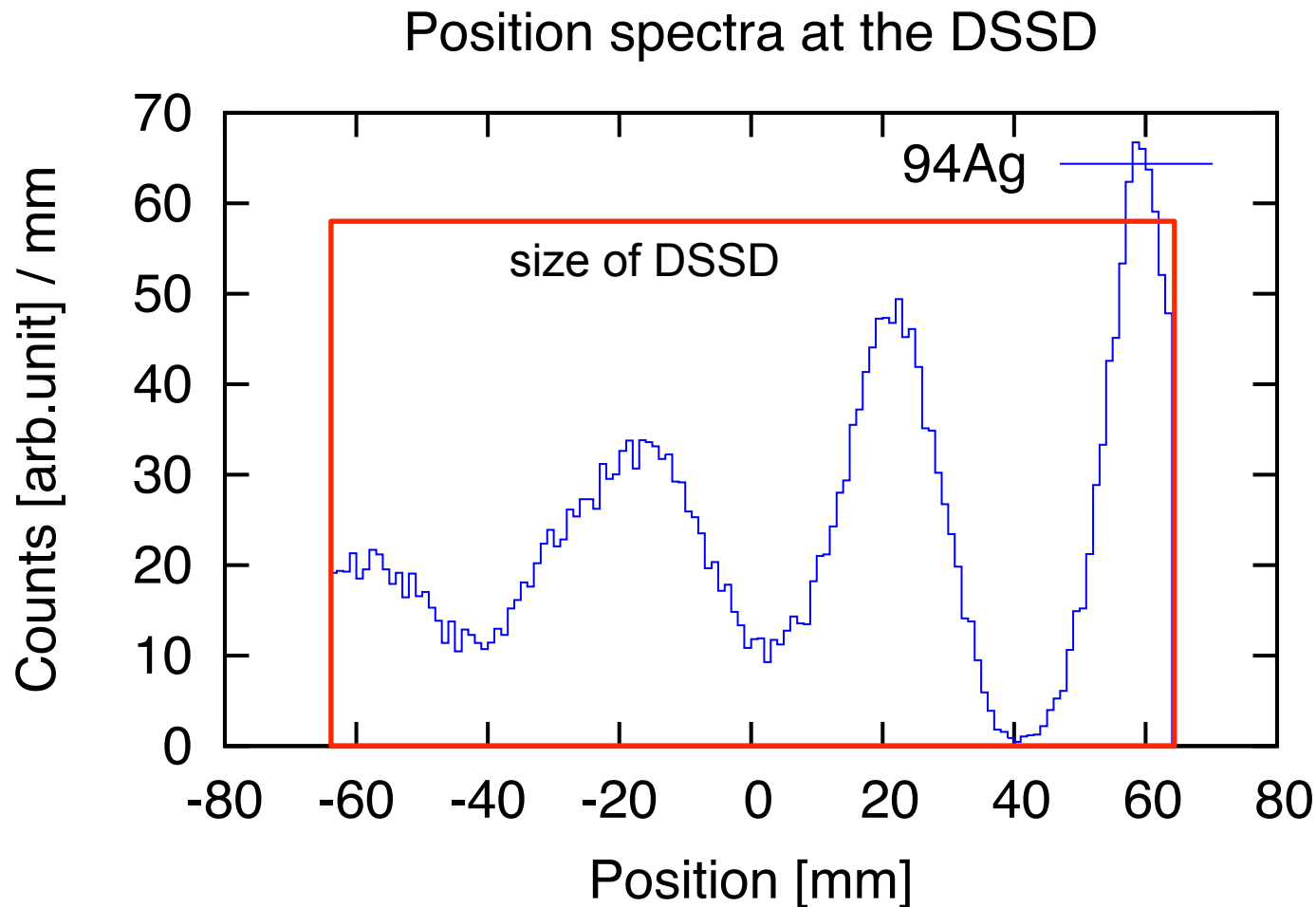
Recoil distributions at the focal plane



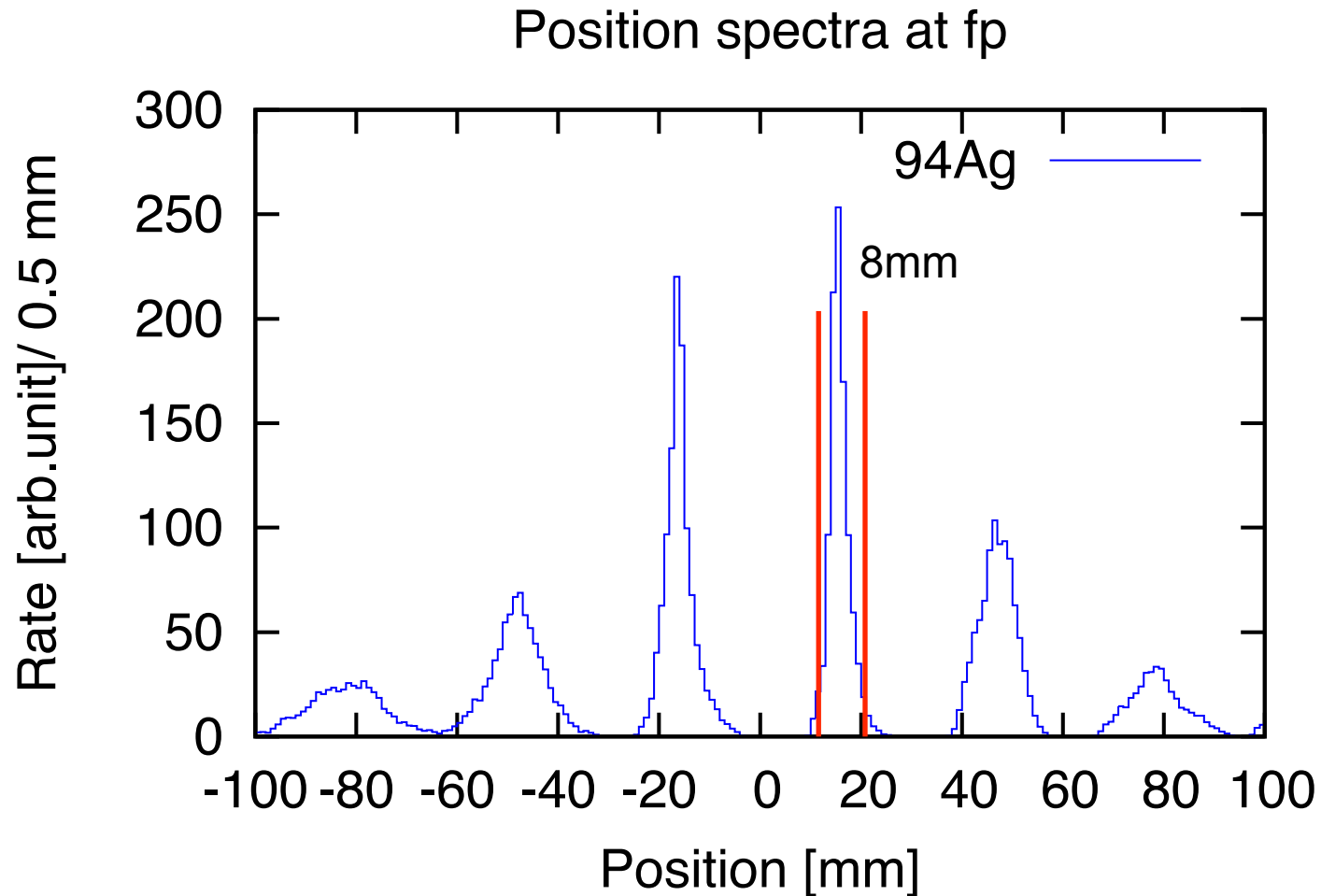
$^{58}\text{Ni}(^{40}\text{Ca}, p3n)^{94}\text{Ag}$ @ 192MeV

Calculations by J. Sarén

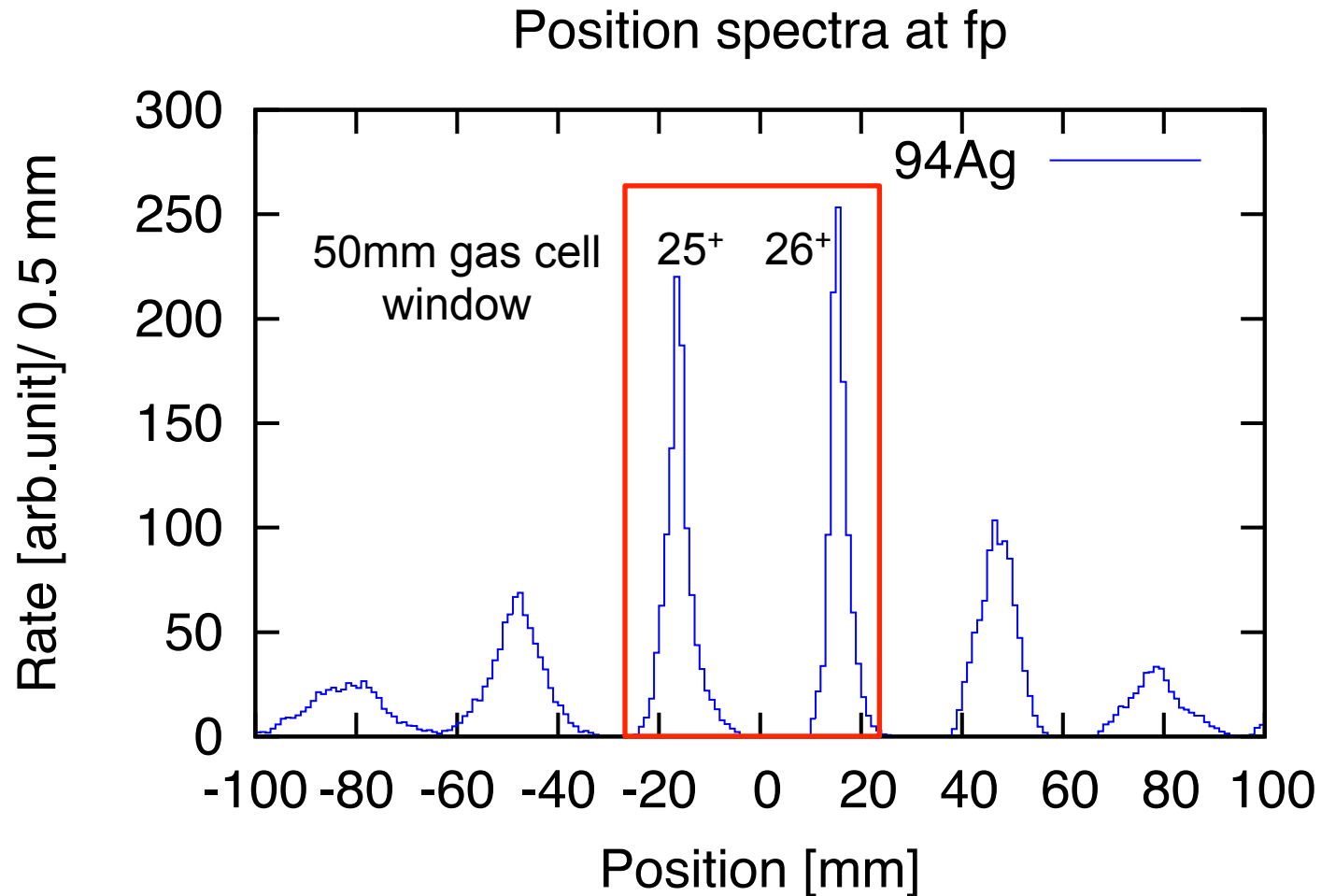
Recoil distributions at the focal plane



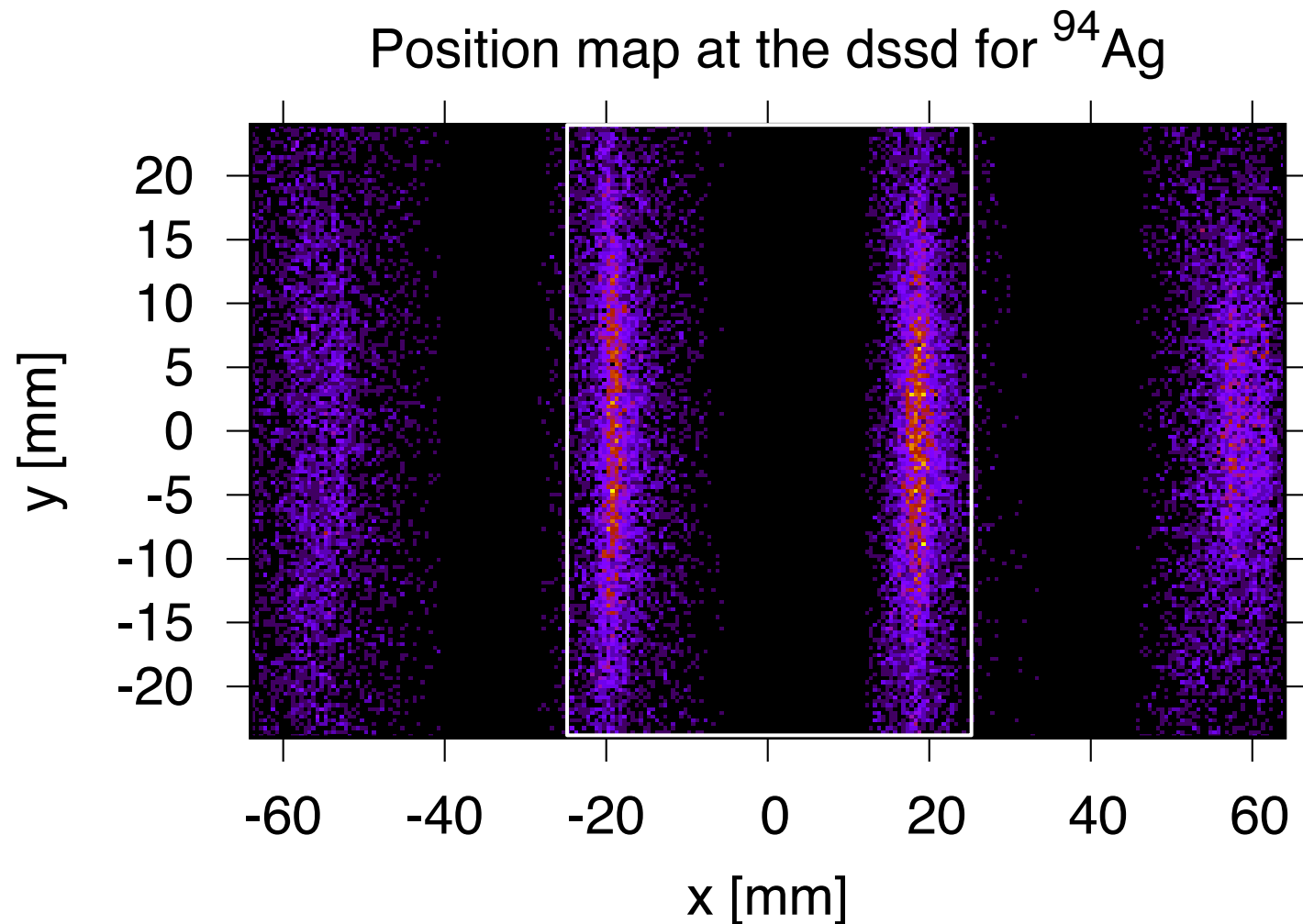
Recoil distributions at the focal plane



Recoil distributions at the focal plane



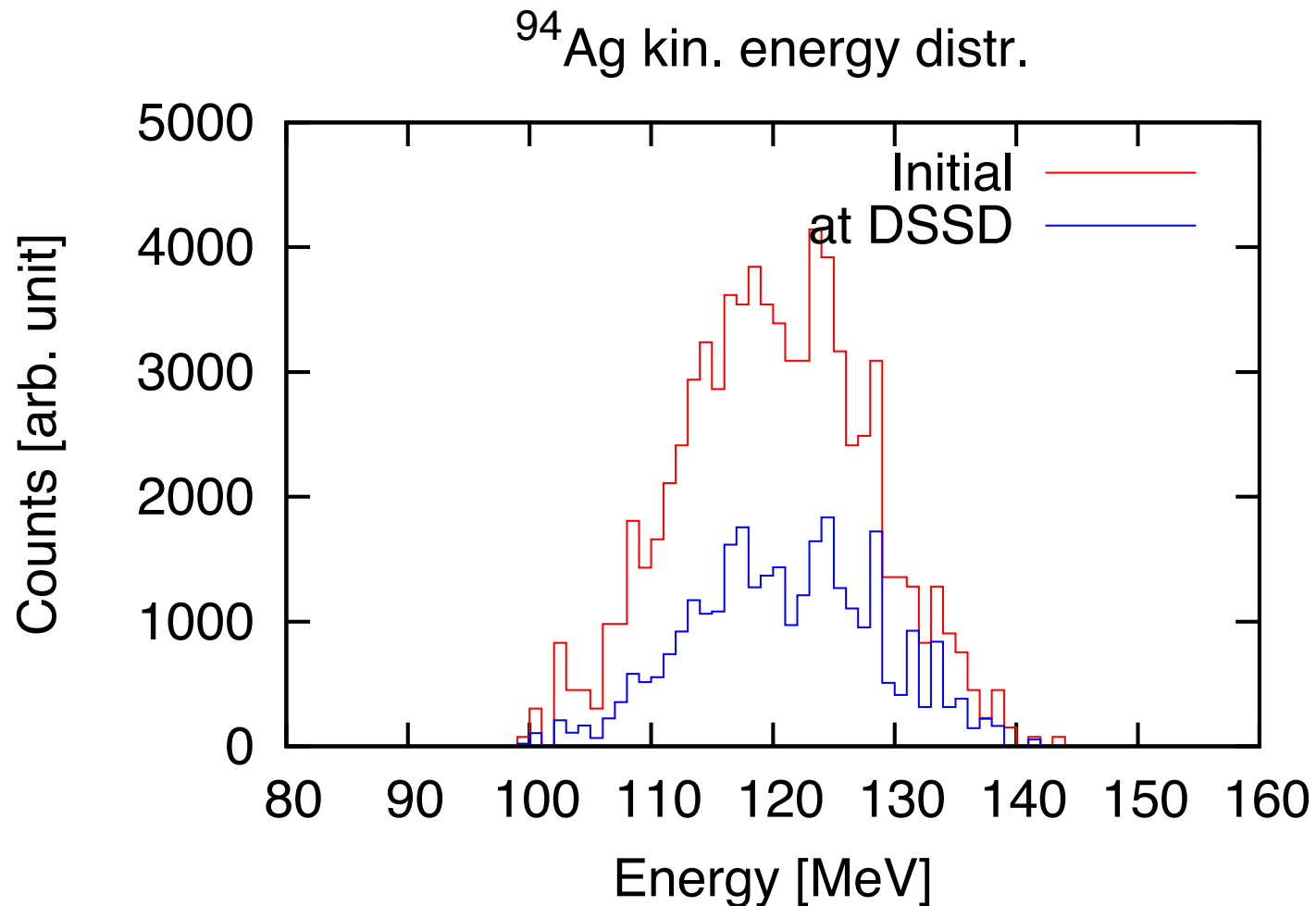
Recoil distributions at the focal plane



$^{58}\text{Ni}(^{40}\text{Ca}, p3n)^{94}\text{Ag}$ @ 192MeV

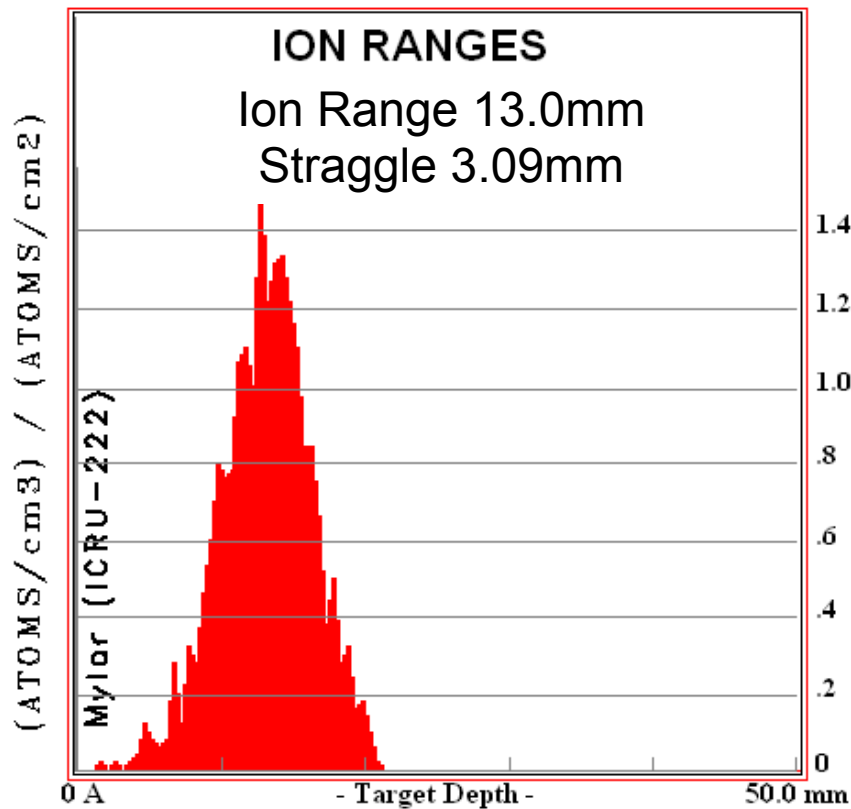
Calculations by J. Sarén

Recoil distributions at the focal plane

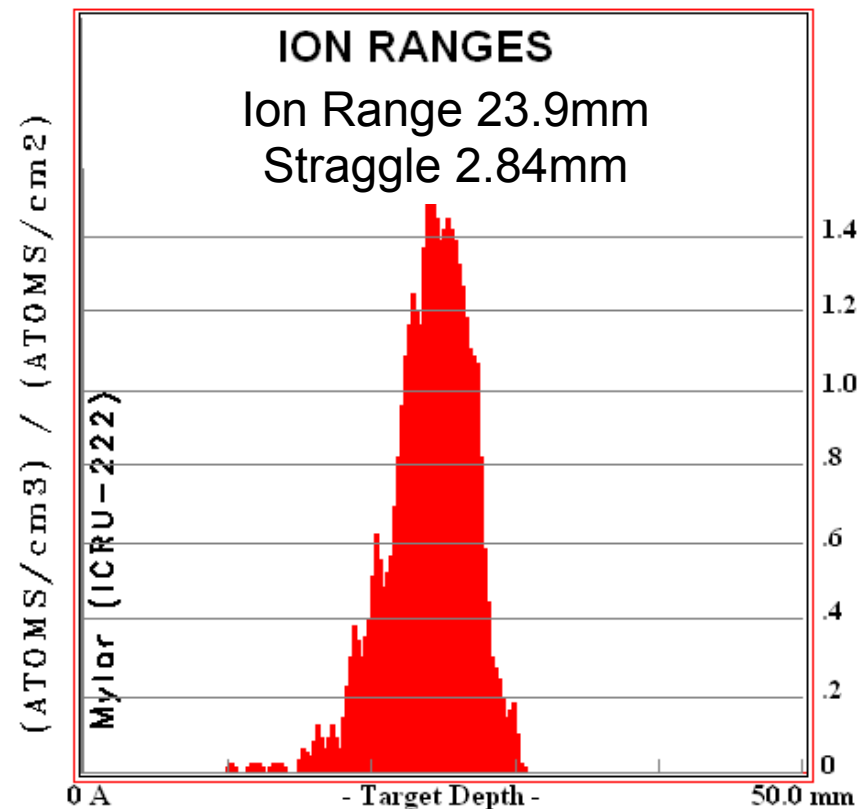


Stopping ranges

$^{58}\text{Ni}(^{40}\text{Ca}, p3n)^{94}\text{Ag}$
 192MeV, 500 $\mu\text{g}/\text{cm}^2$
 10+1 μm Mylar foils, 500mbar **Ar**

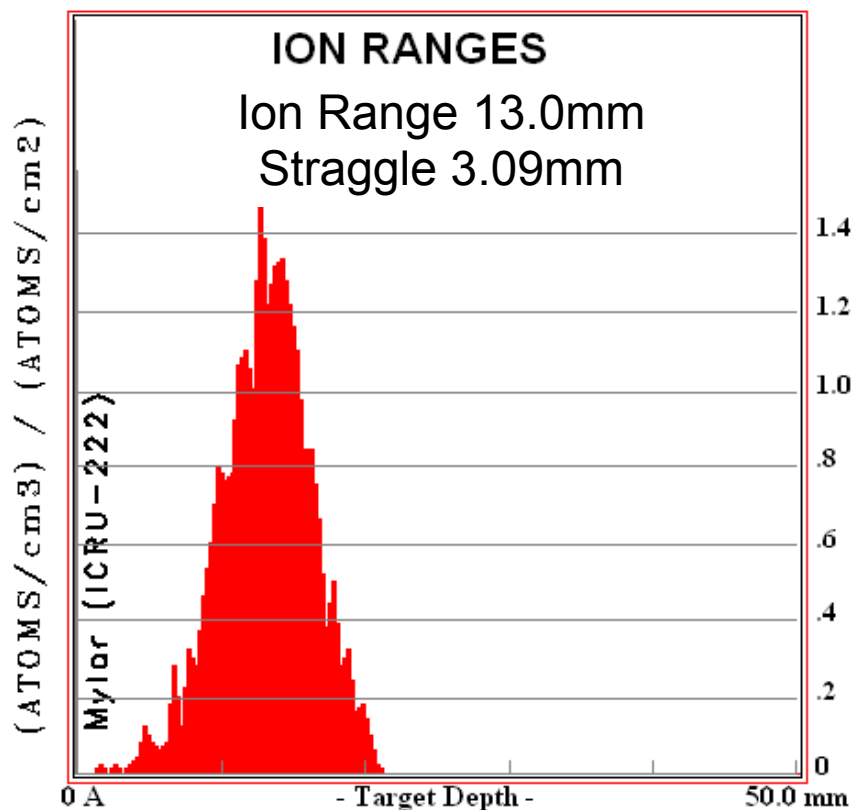


$^{40}\text{Ca}(^{58}\text{Ni}, p3n)^{94}\text{Ag}$
 240MeV, 500 $\mu\text{g}/\text{cm}^2$
 10+1 μm Mylar foils, 500mbar **Ar**

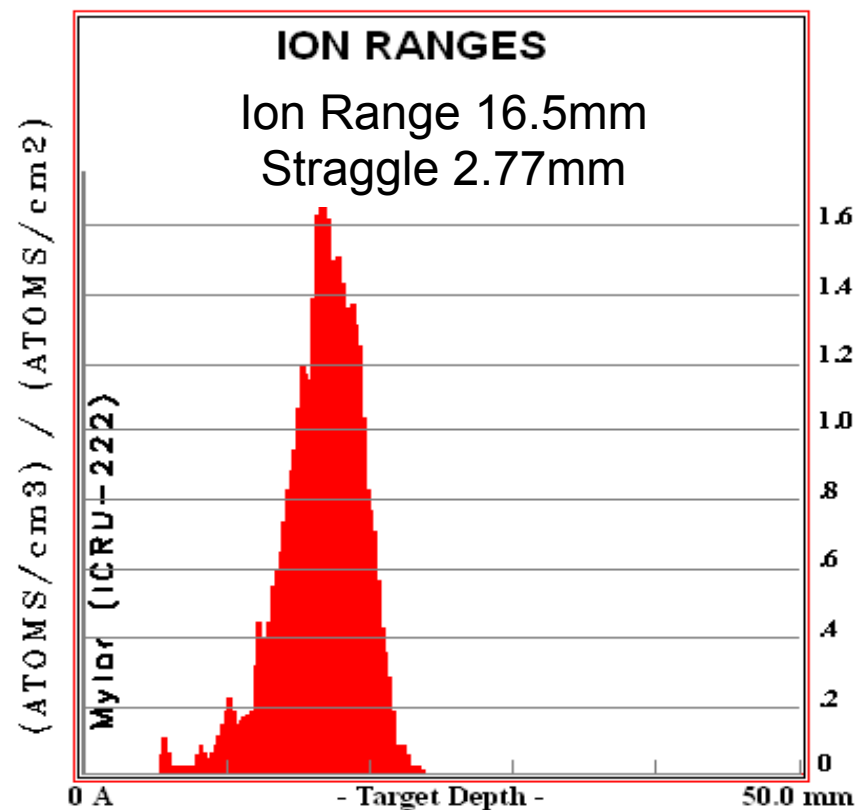


Stopping ranges

$^{58}\text{Ni}(^{40}\text{Ca},\text{p}3\text{n})^{94}\text{Ag}$
 192MeV, 500 $\mu\text{g}/\text{cm}^2$
 10+1 μm Mylar foils, 500mbar **Ar**

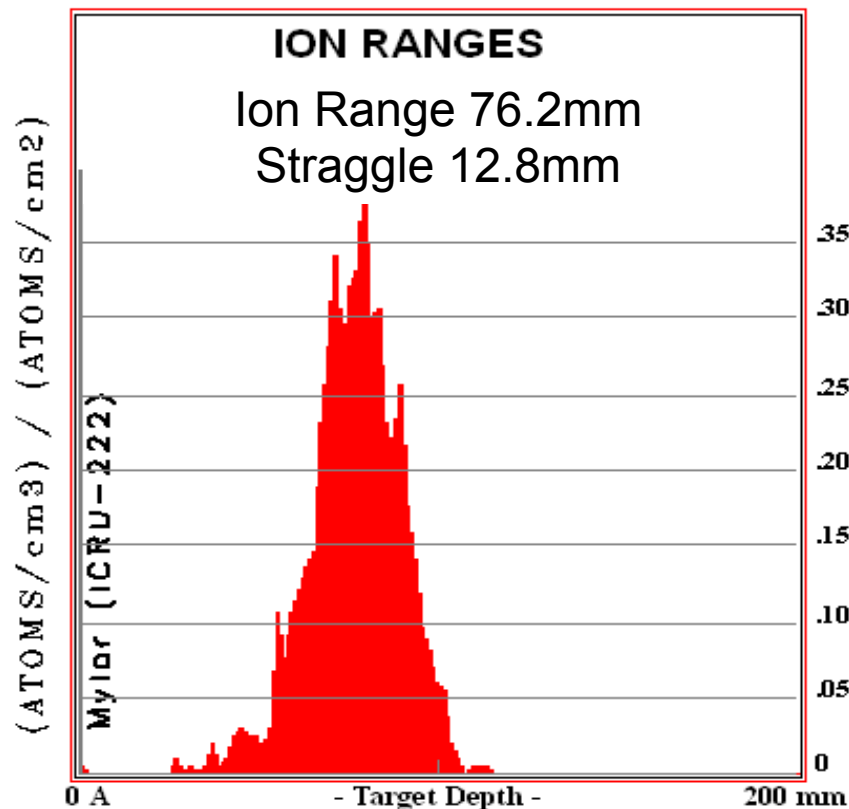


$^{40}\text{Ca}(^{58}\text{Ni},\text{p}3\text{n})^{94}\text{Ag}$
 240MeV, 500 $\mu\text{g}/\text{cm}^2$
 13+1 μm Mylar foils, 500mbar **Ar**

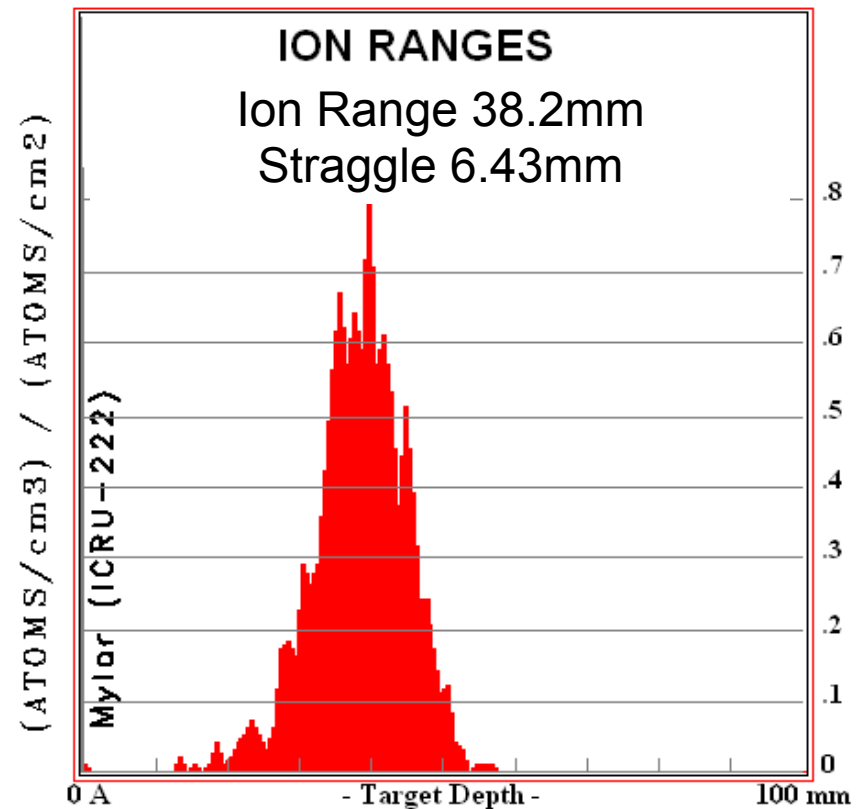


Stopping ranges

$^{58}\text{Ni}(^{40}\text{Ca},\text{p}3\text{n})^{94}\text{Ag}$
 192MeV, 500 $\mu\text{g}/\text{cm}^2$
 10+1 μm Mylar foils, 500mbar **He**

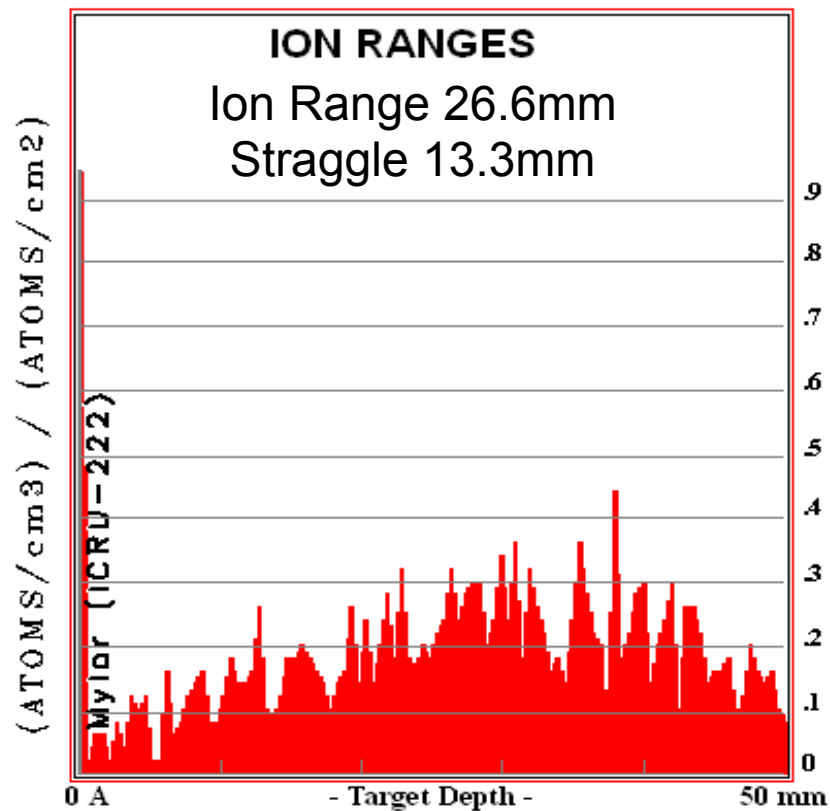


$^{58}\text{Ni}(^{40}\text{Ca},\text{p}3\text{n})^{94}\text{Ag}$
 192MeV, 500 $\mu\text{g}/\text{cm}^2$
 10+1 μm Mylar foil, 1000mbar **He**

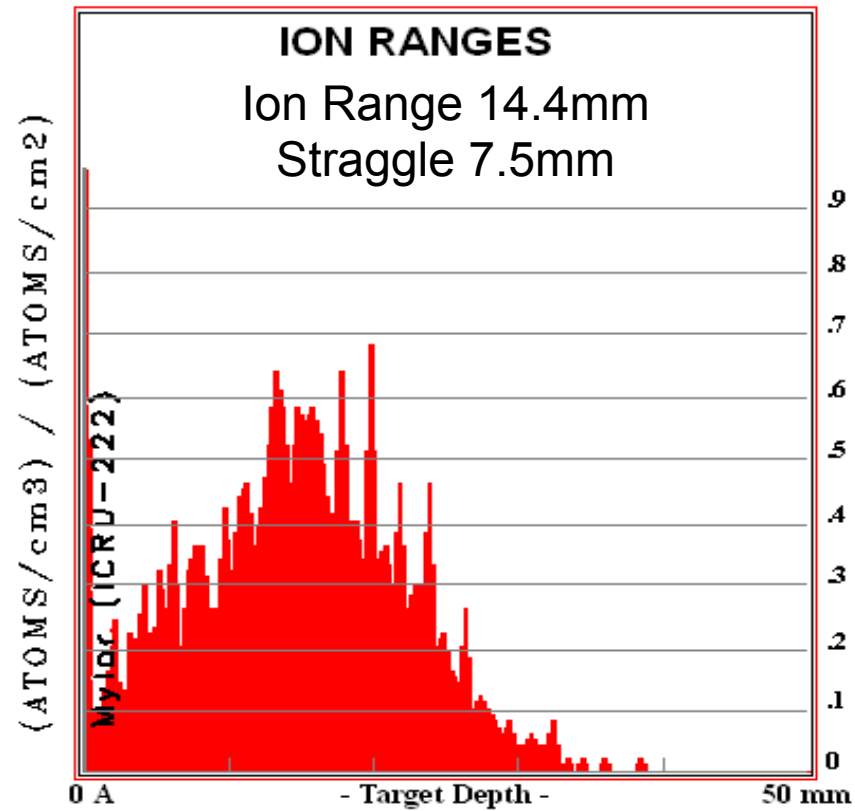


Stopping ranges

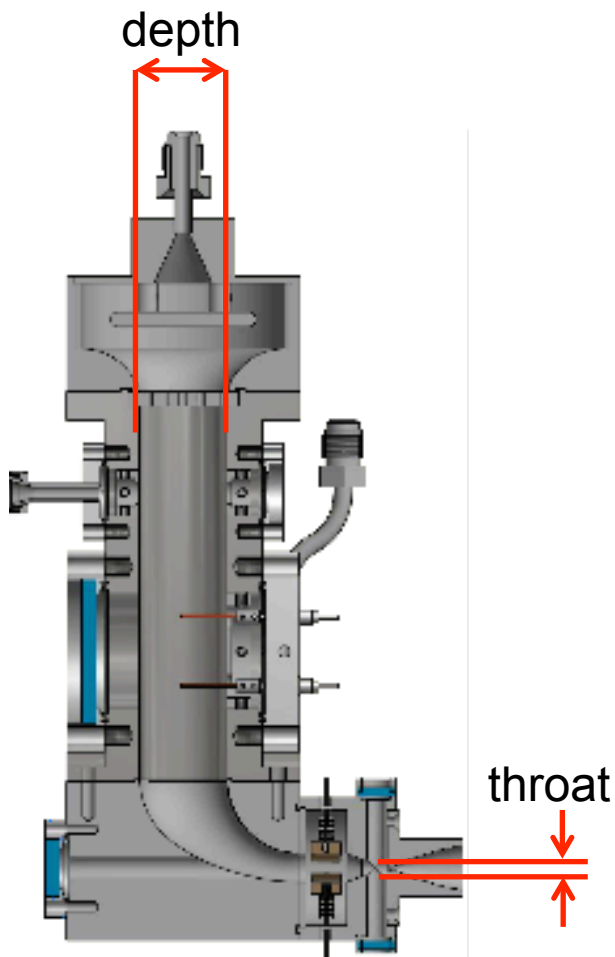
$^{58}\text{Ni}(^{40}\text{Ca},\text{p}3\text{n})^{94}\text{Ag}$
192MeV, 500 $\mu\text{g}/\text{cm}^2$
14 μm Mylar foils, 500mbar **He**



$^{58}\text{Ni}(^{40}\text{Ca},\text{p}3\text{n})^{94}\text{Ag}$
192MeV, 500 $\mu\text{g}/\text{cm}^2$
14 μm Mylar foil, 1000mbar **He**



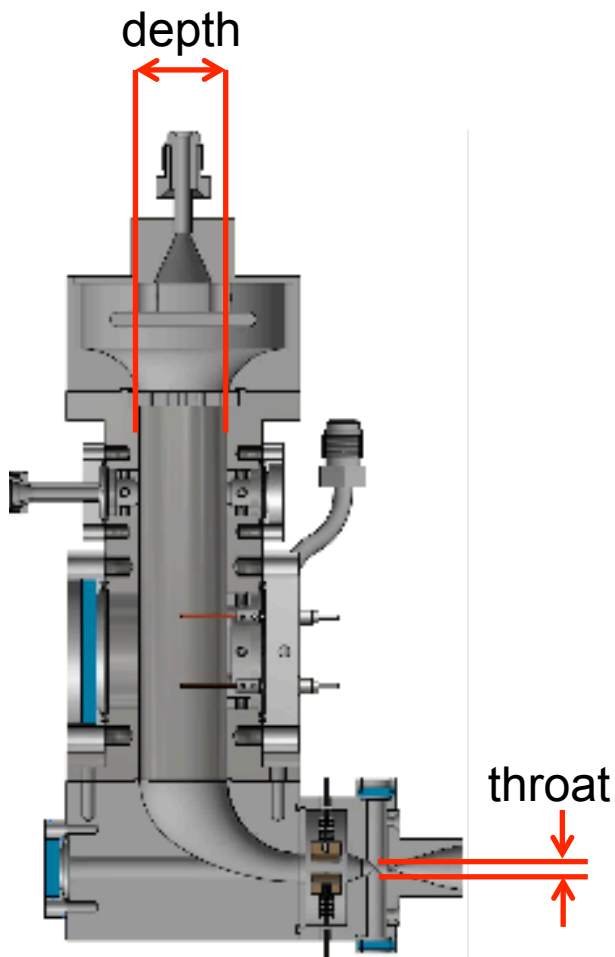
Evacuation times



For Ar:

- Depth: 30mm. Throat: 1mm (1.5mm)
 - By detailed calculation of the gas velocity profile in the cell: 630ms *
 - By estimating the evacuation time: ~600ms (~260ms)
- Depth: 20mm. Throat: 1.5mm
 - By detailed calculation of the gas velocity profile in the cell: 190ms *
 - By estimating the evacuation time: ~180ms

Evacuation times



For Ar:

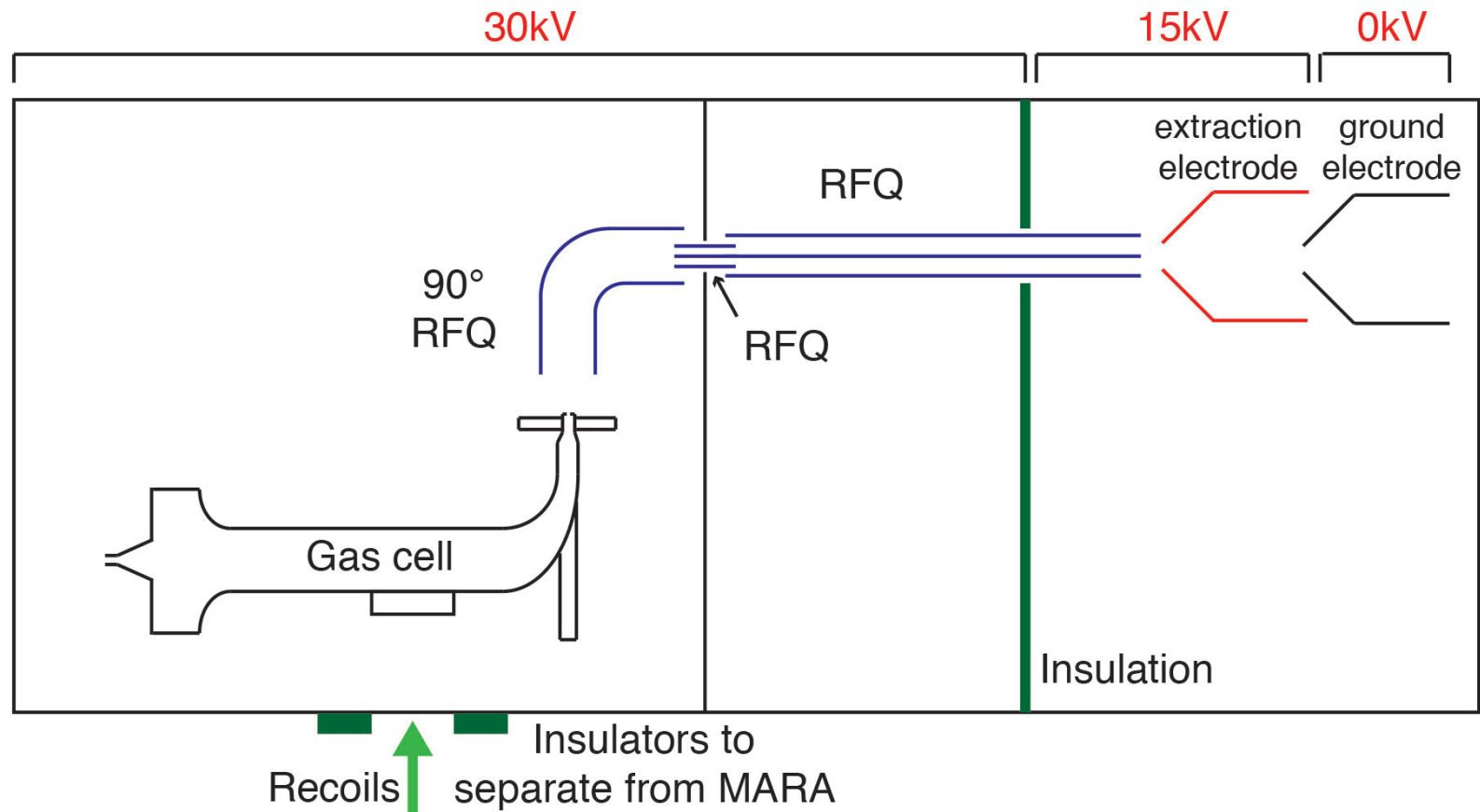
- Depth: 30mm. Throat: 1mm (1.5mm)
 - By detailed calculation of the gas velocity profile in the cell: 630ms *
 - By estimating the evacuation time: ~600ms (~260ms)
- Depth: 20mm. Throat: 1.5mm
 - By detailed calculation of the gas velocity profile in the cell: 190ms *
 - By estimating the evacuation time: ~180ms

For He:

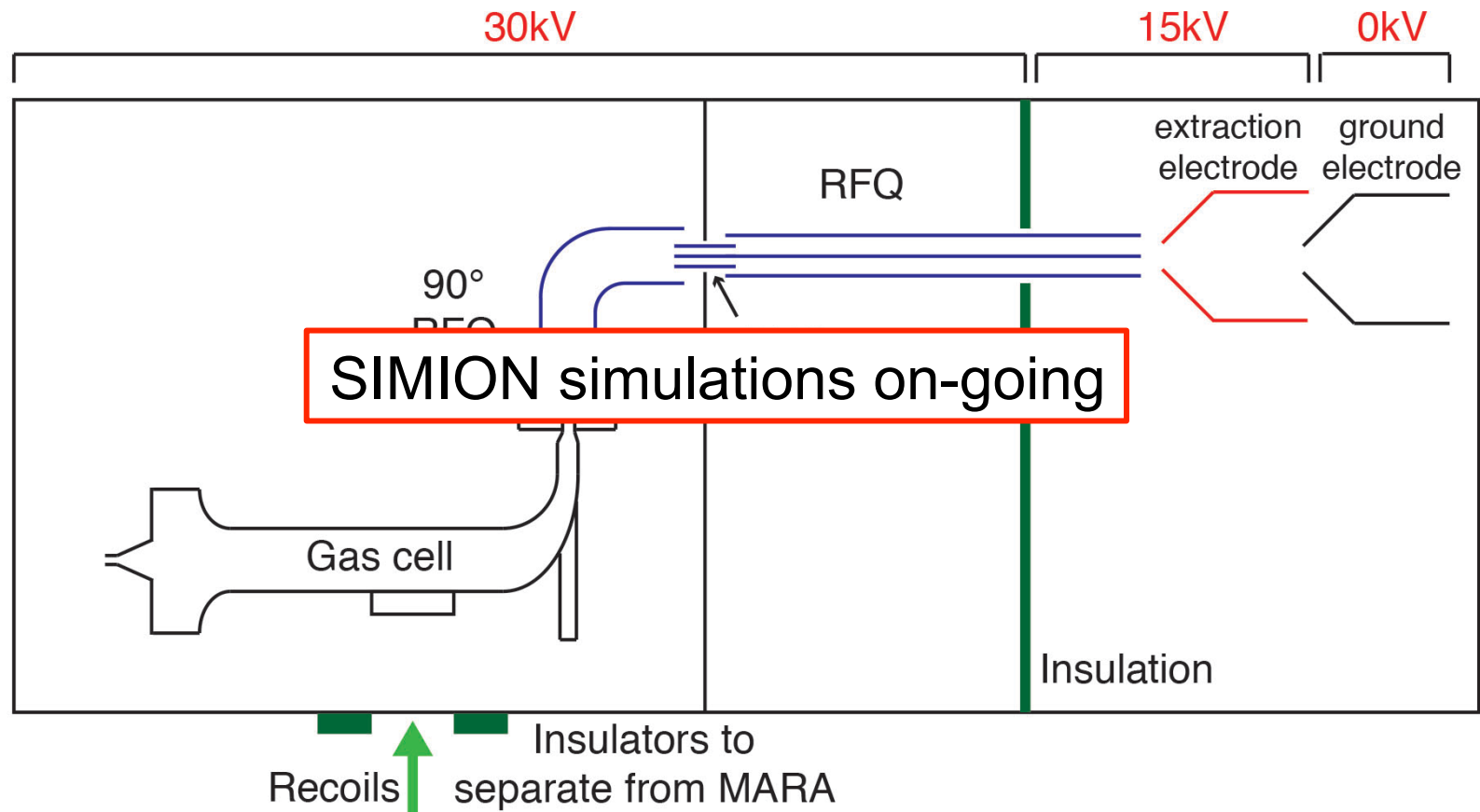
- Depth: 30mm. Throat: 1mm
 - By estimating the evacuation time: ~180ms
- Depth: 20mm. Throat: 1.5mm
 - By estimating the evacuation time: ~60ms

*Yu. Kudryavtsev *et al.*, Nucl. Instr. and Meth. B **376**, 345 (2016)

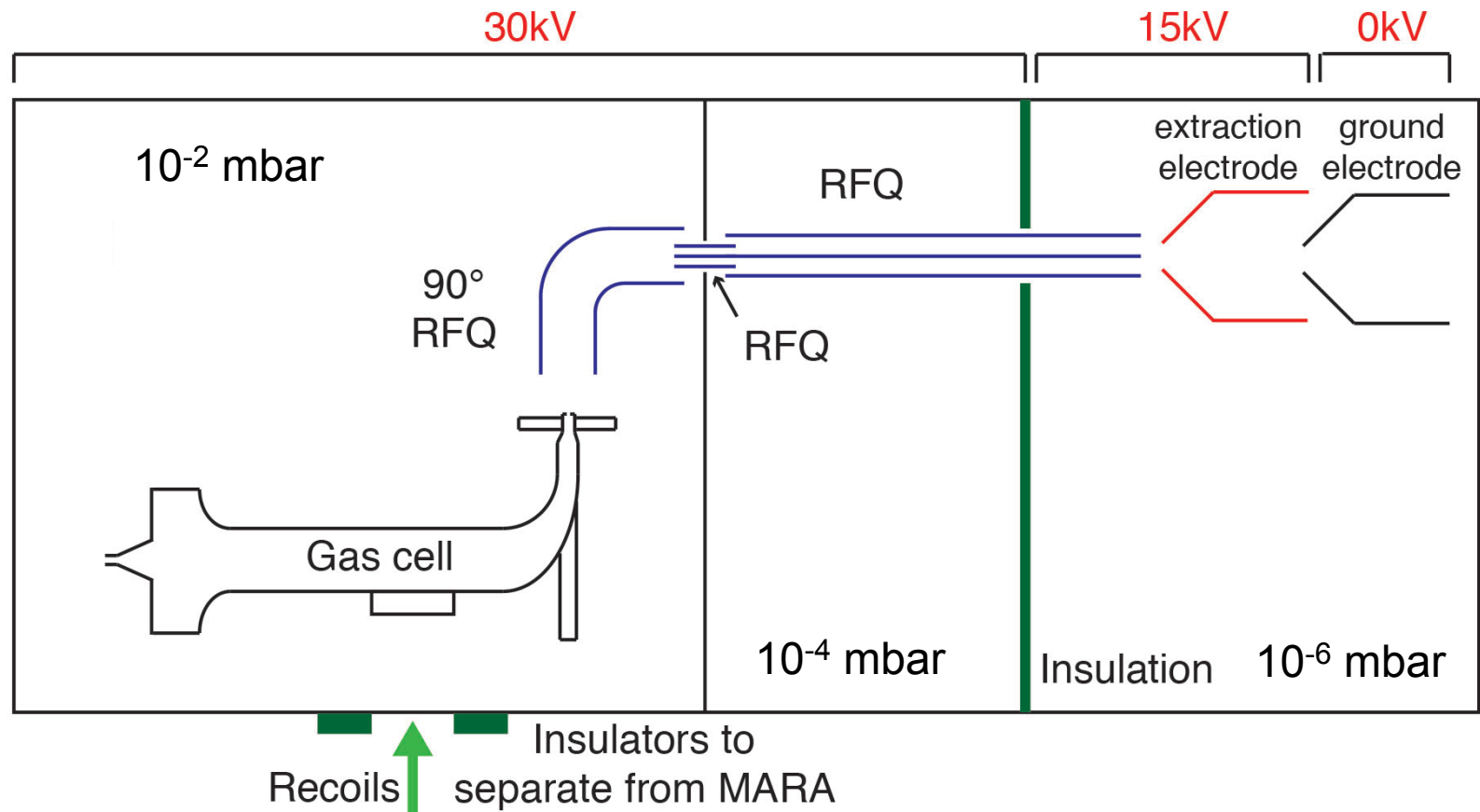
Ion Extraction



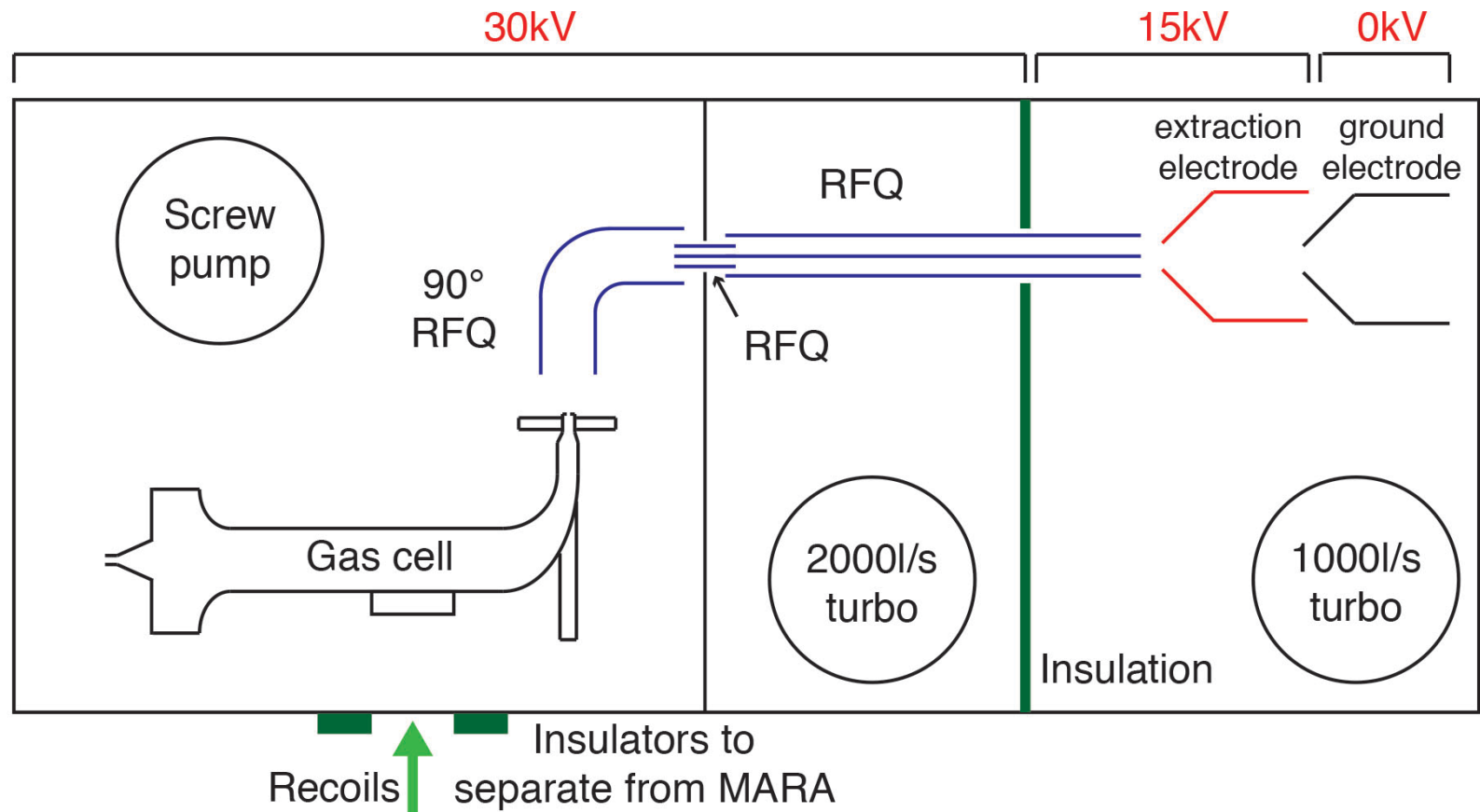
Ion Extraction



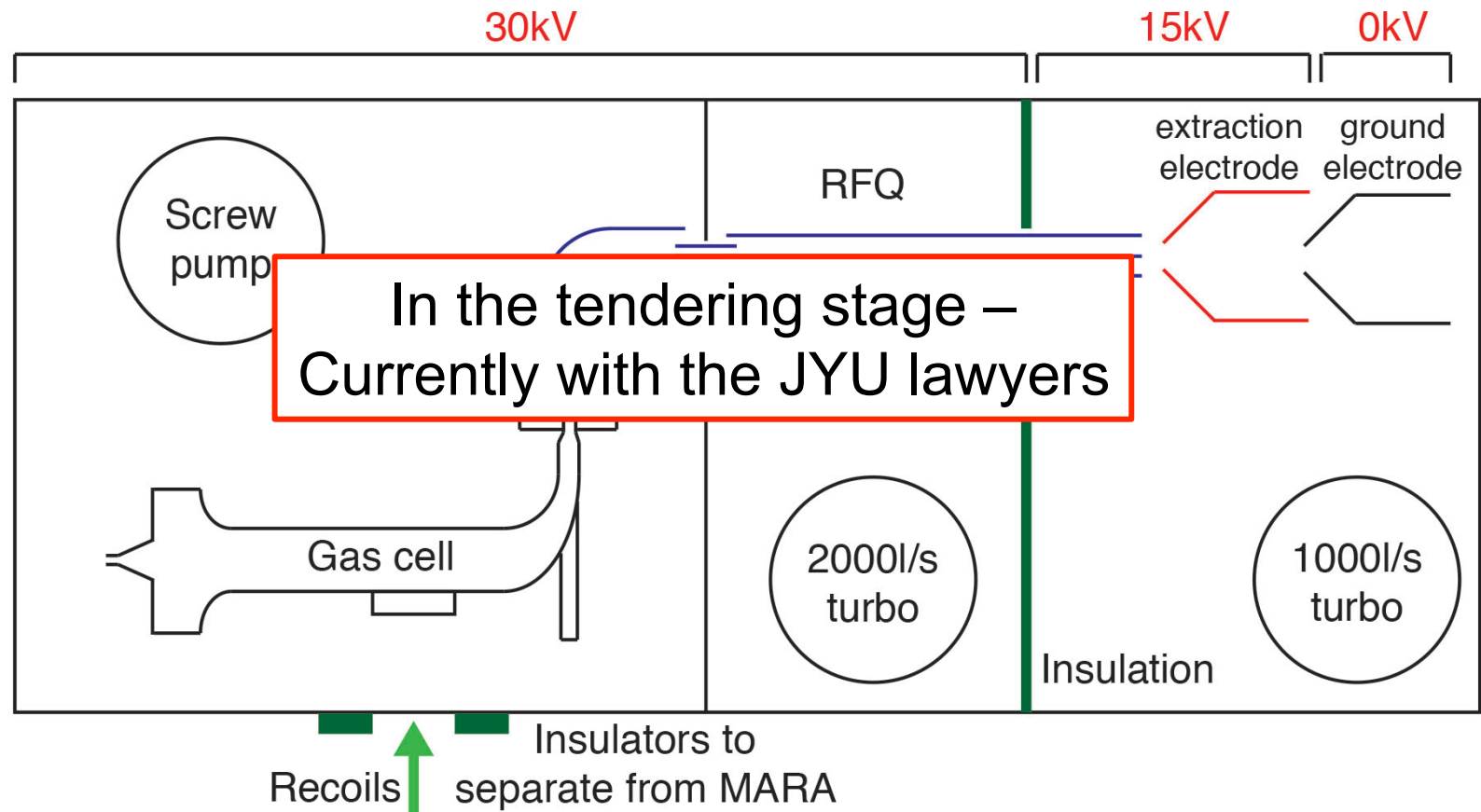
Differential pumping



Differential pumping

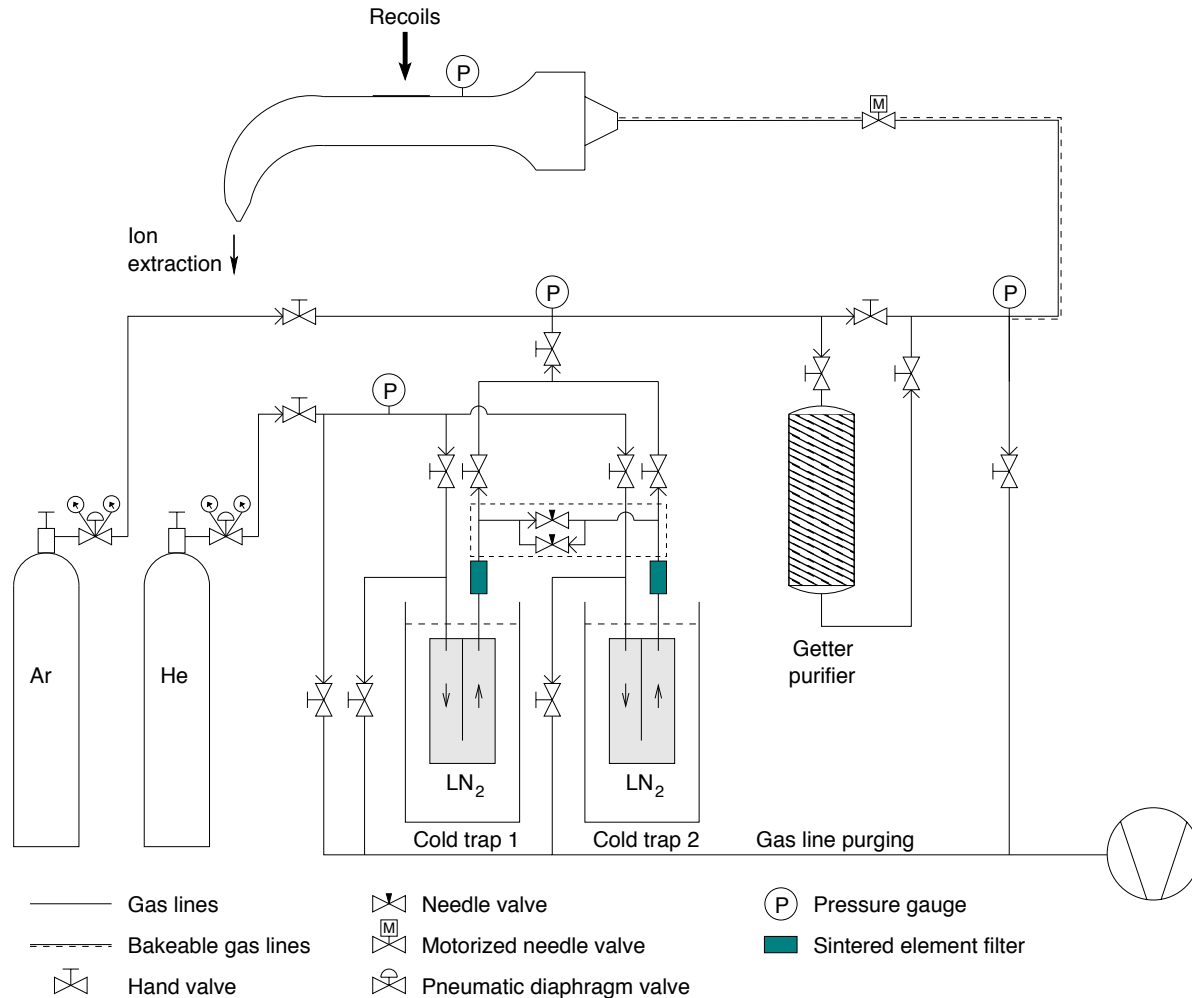


Differential pumping



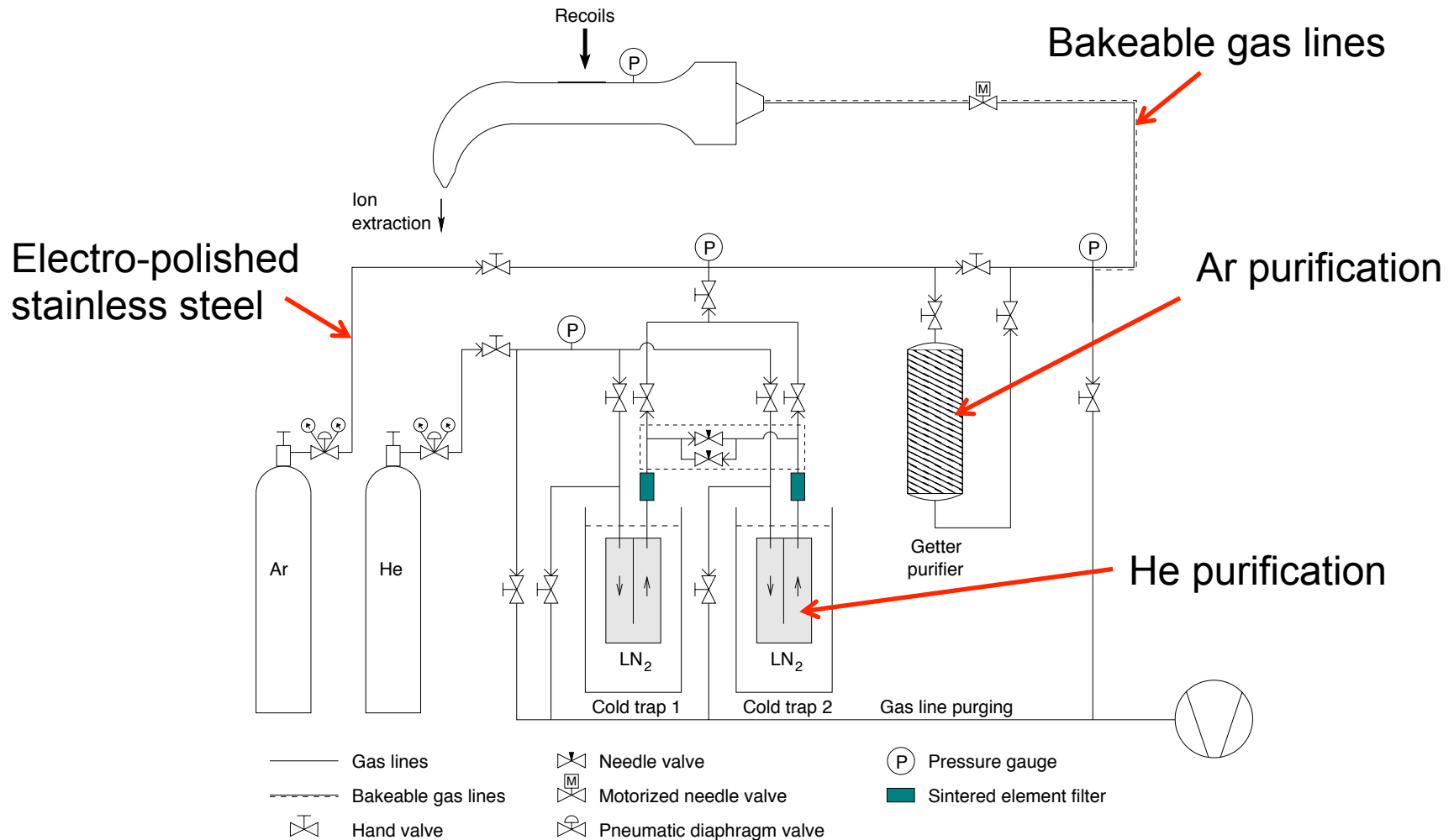
Gas handling system

Based on the system build for IGISOL-4 by I. Pohjalainen



Gas handling system

Based on the system build for IGISOL-4 by I. Pohjalainen

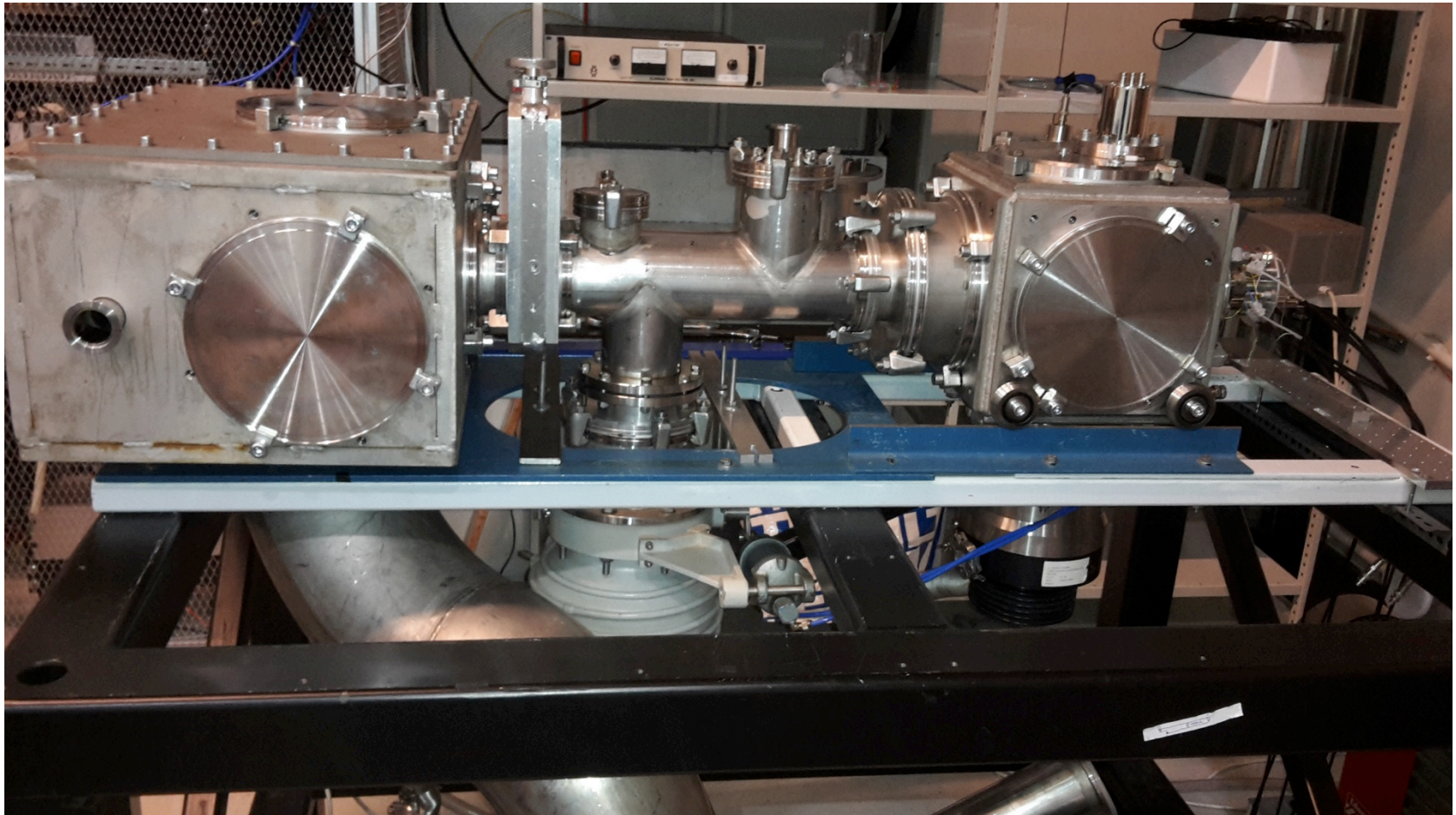


Gas handling system



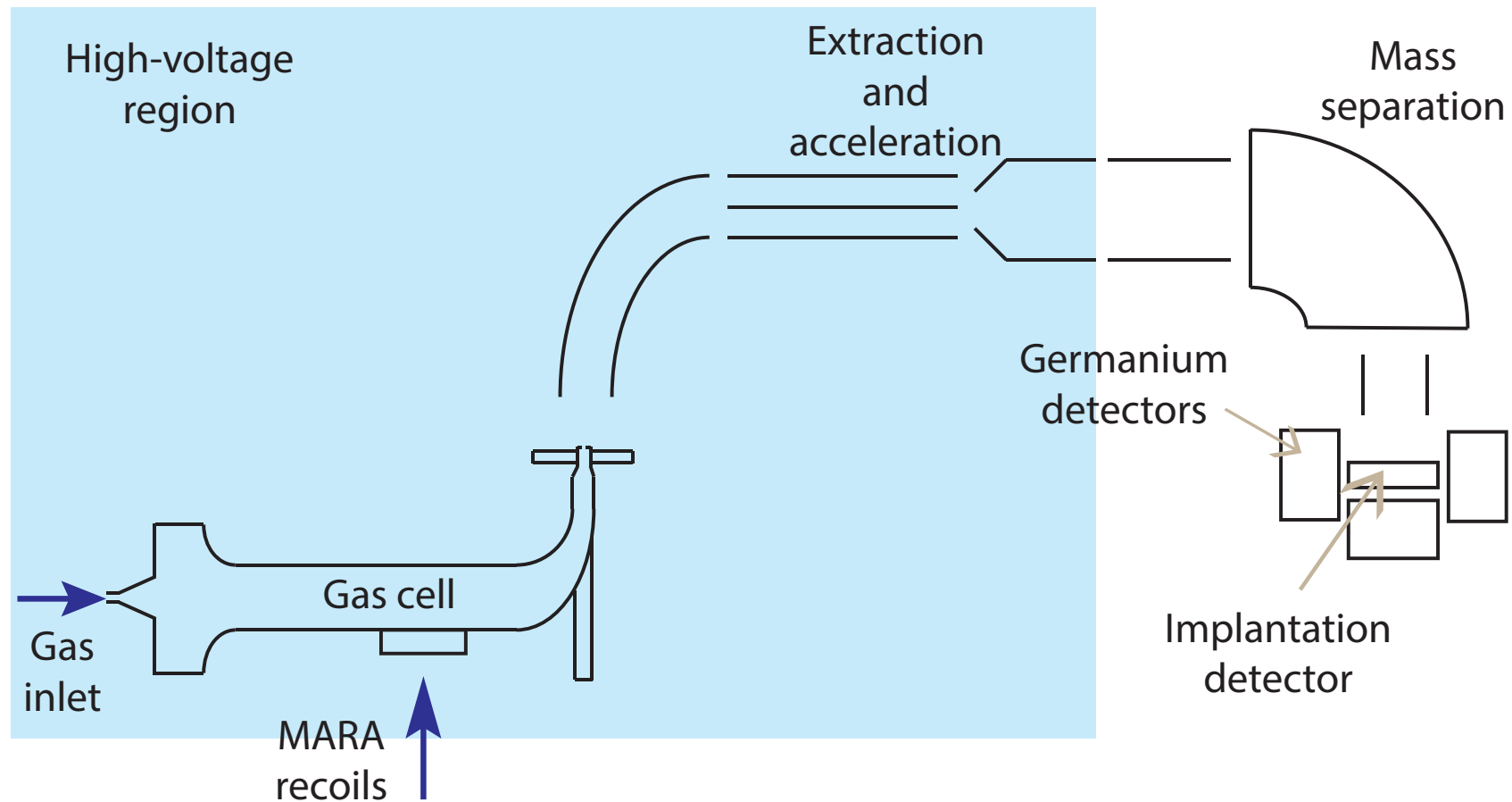
MonoTorr PS4-MT3-R2
Heated getter purifier

IGISOL off-line rig – Equipment testing



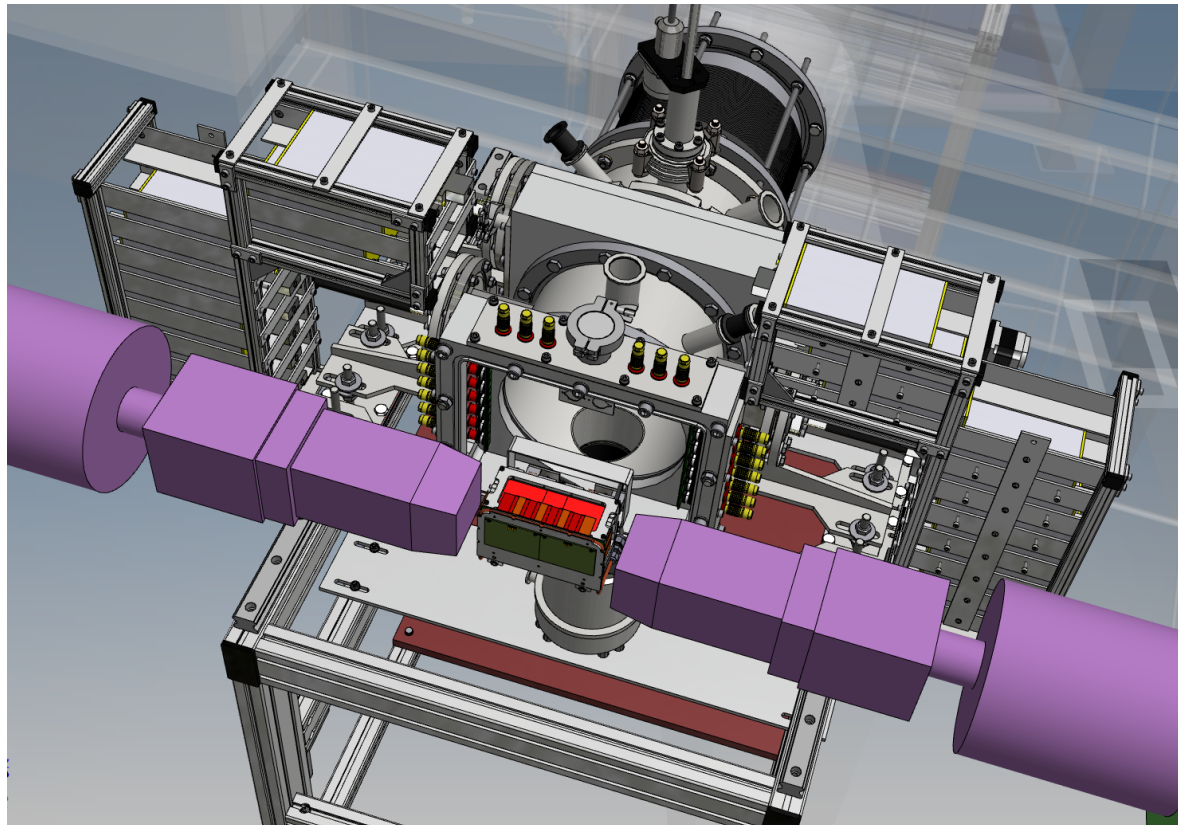
Detector stations

■ 1st phase



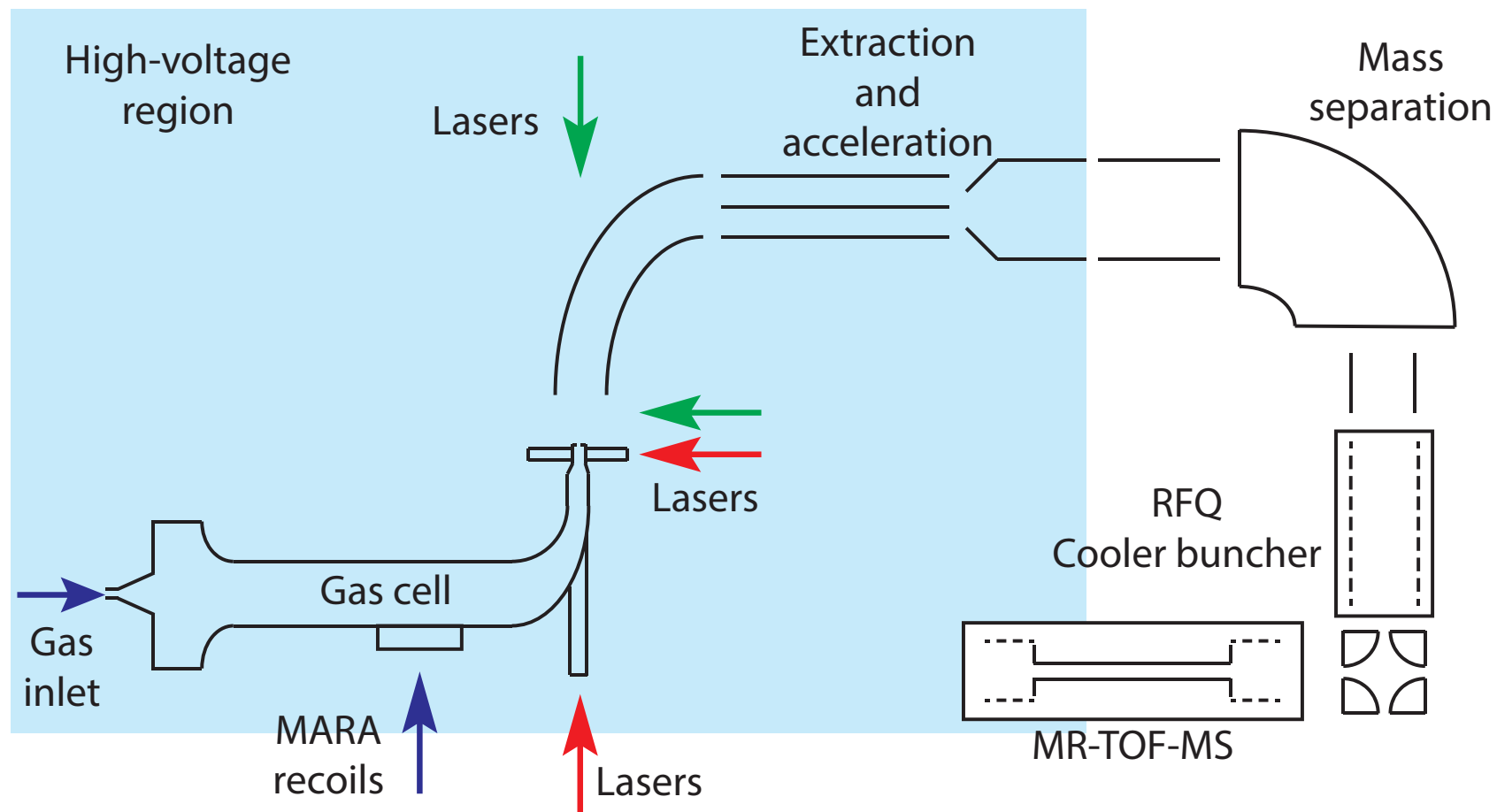
Detector stations

- 1st phase



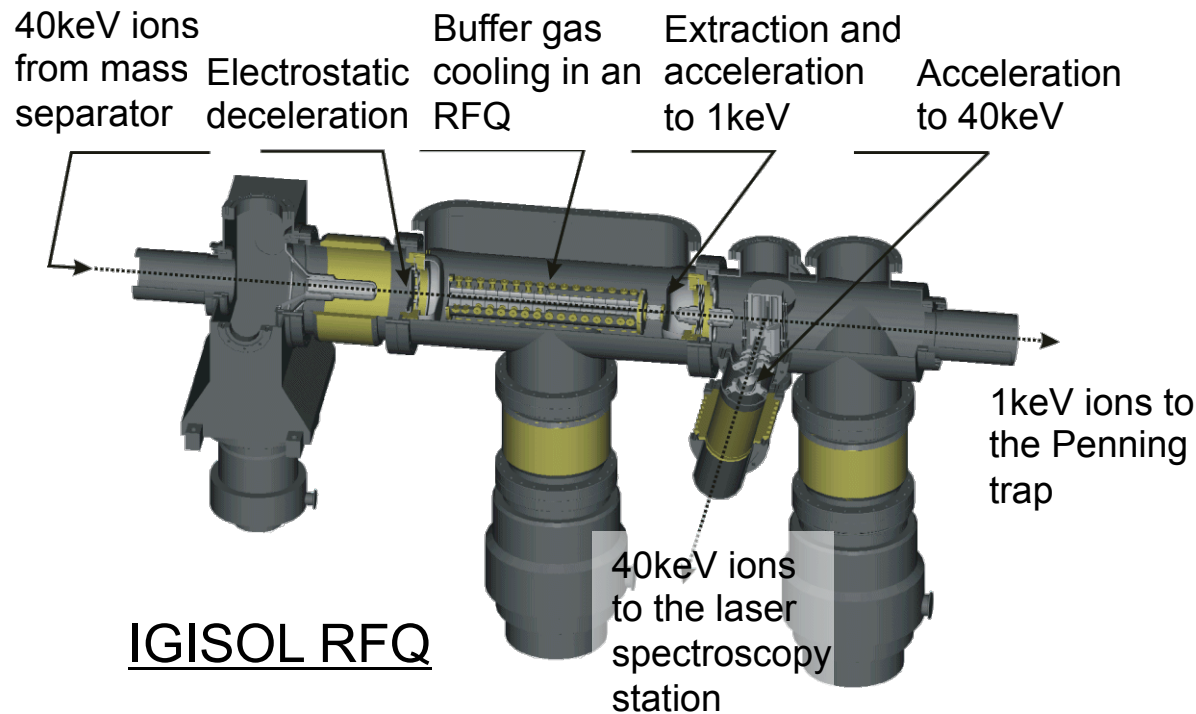
Detector stations

■ 2nd phase



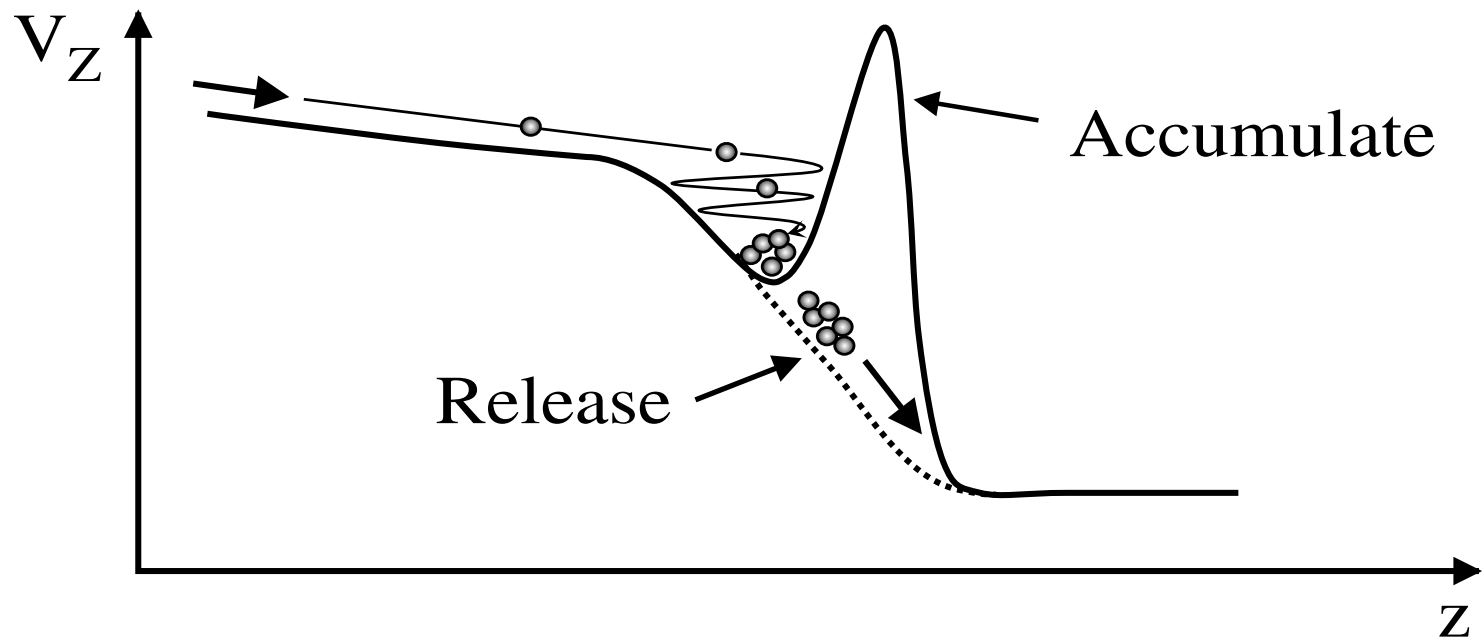
Radiofrequency quadrupole cooler and buncher

To be used for decelerating, cooling and bunching of the ion beam to make it suitable for the MR-TOF mass spectrometer.

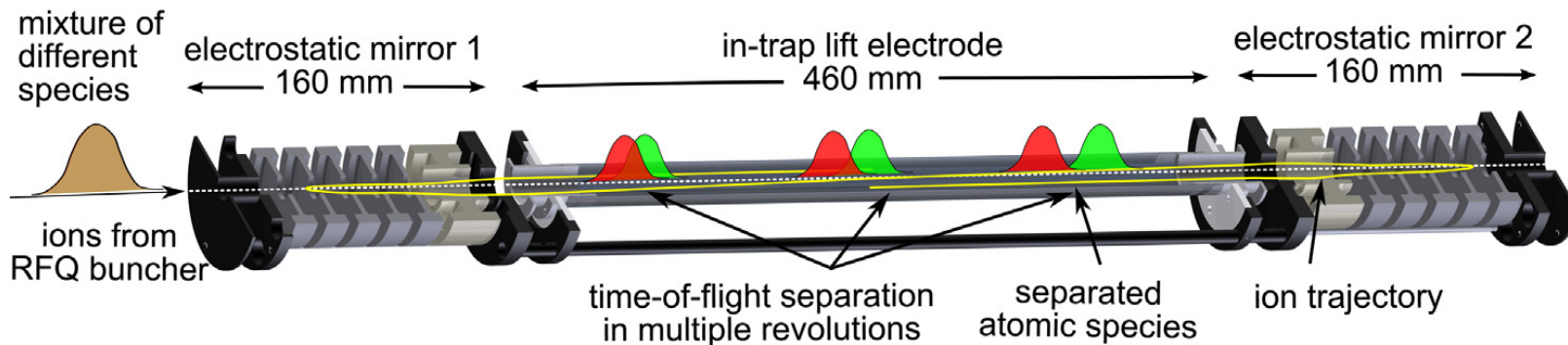


Radiofrequency quadrupole cooler and buncher

To be used for decelerating, cooling and bunching of the beam to make it suitable for the MR-TOF mass spectrometer.



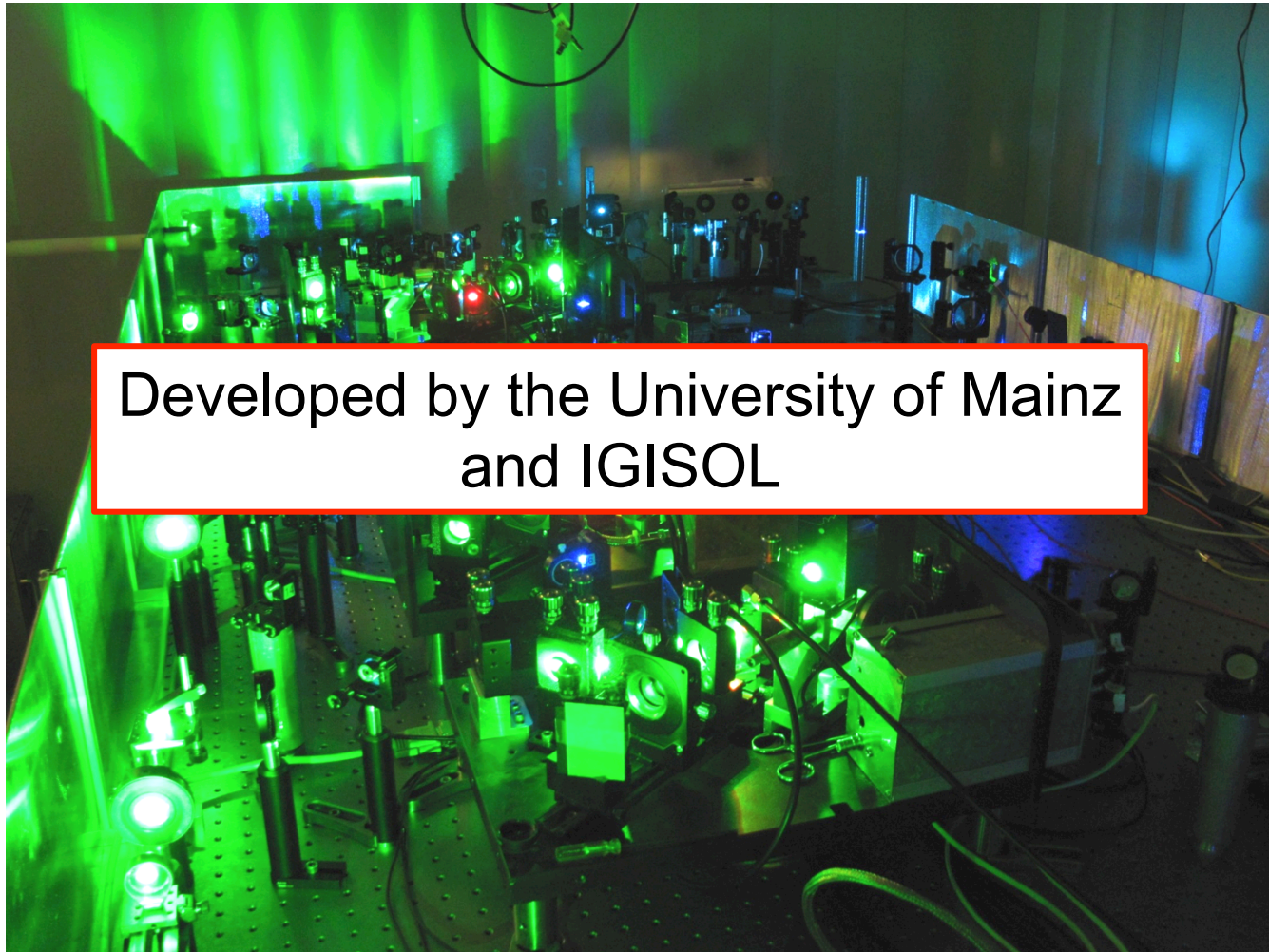
Multi-reflection time-of-flight mass analyser



Lasers system

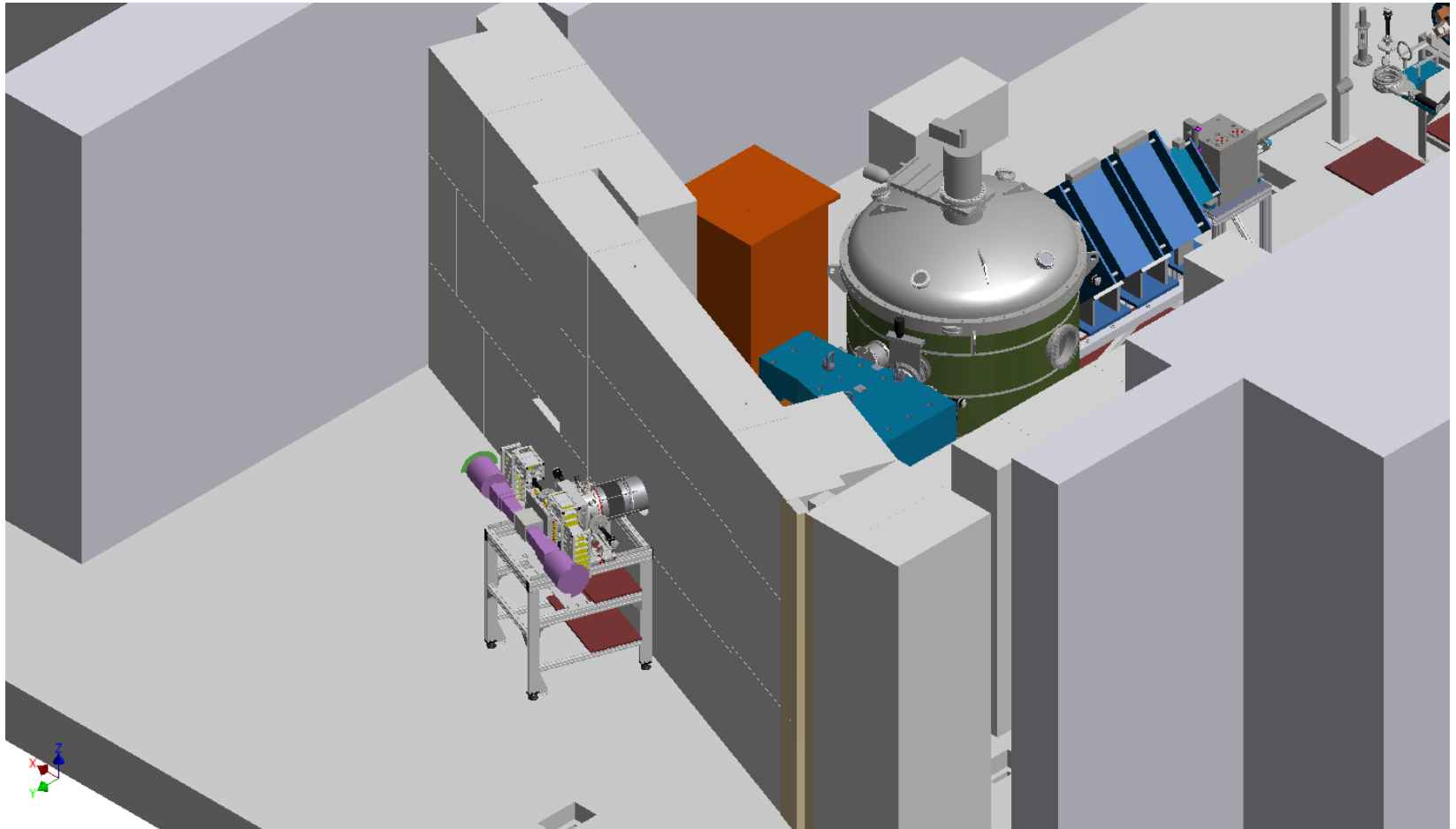


Lasers system

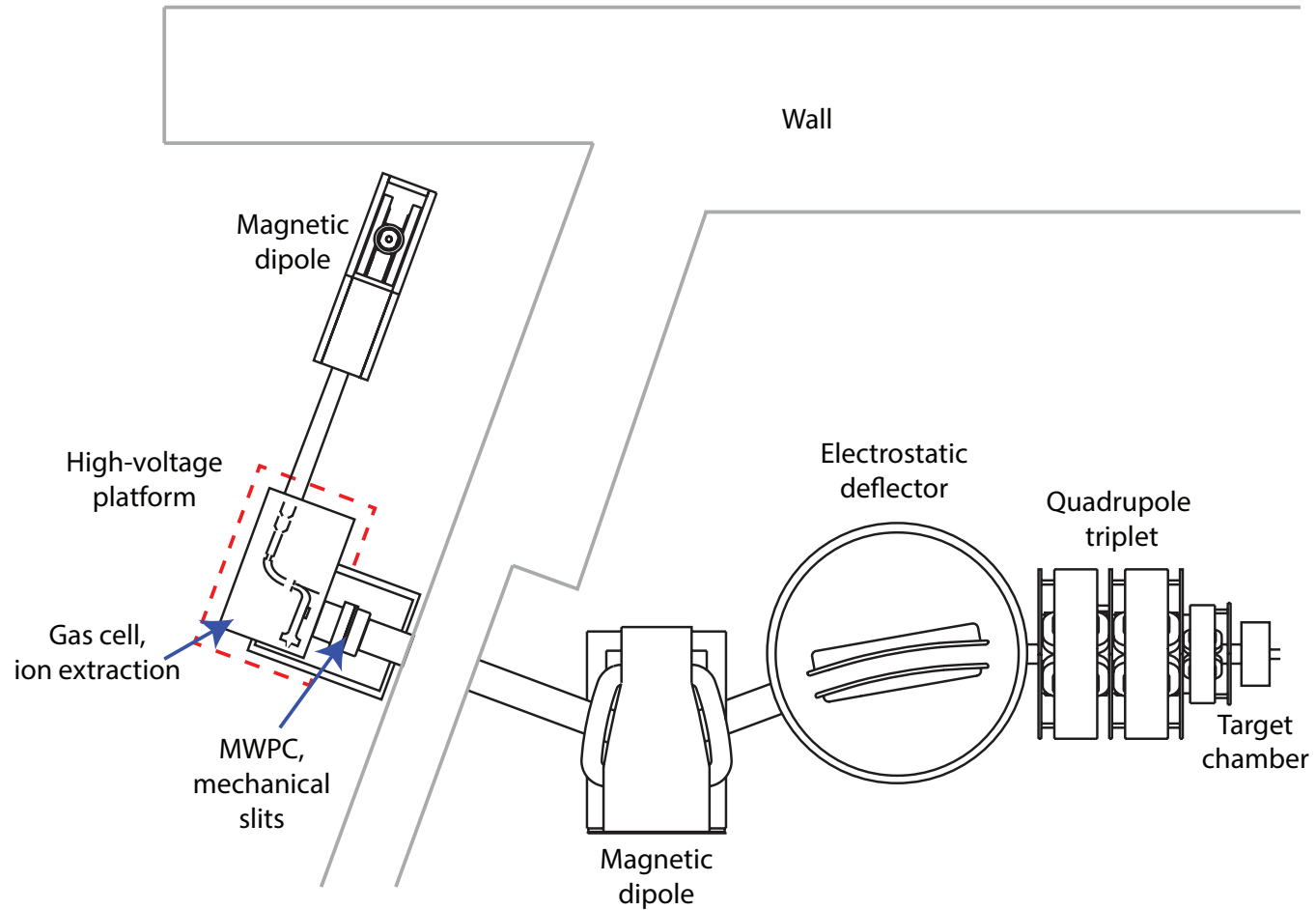


Developed by the University of Mainz
and IGISOL

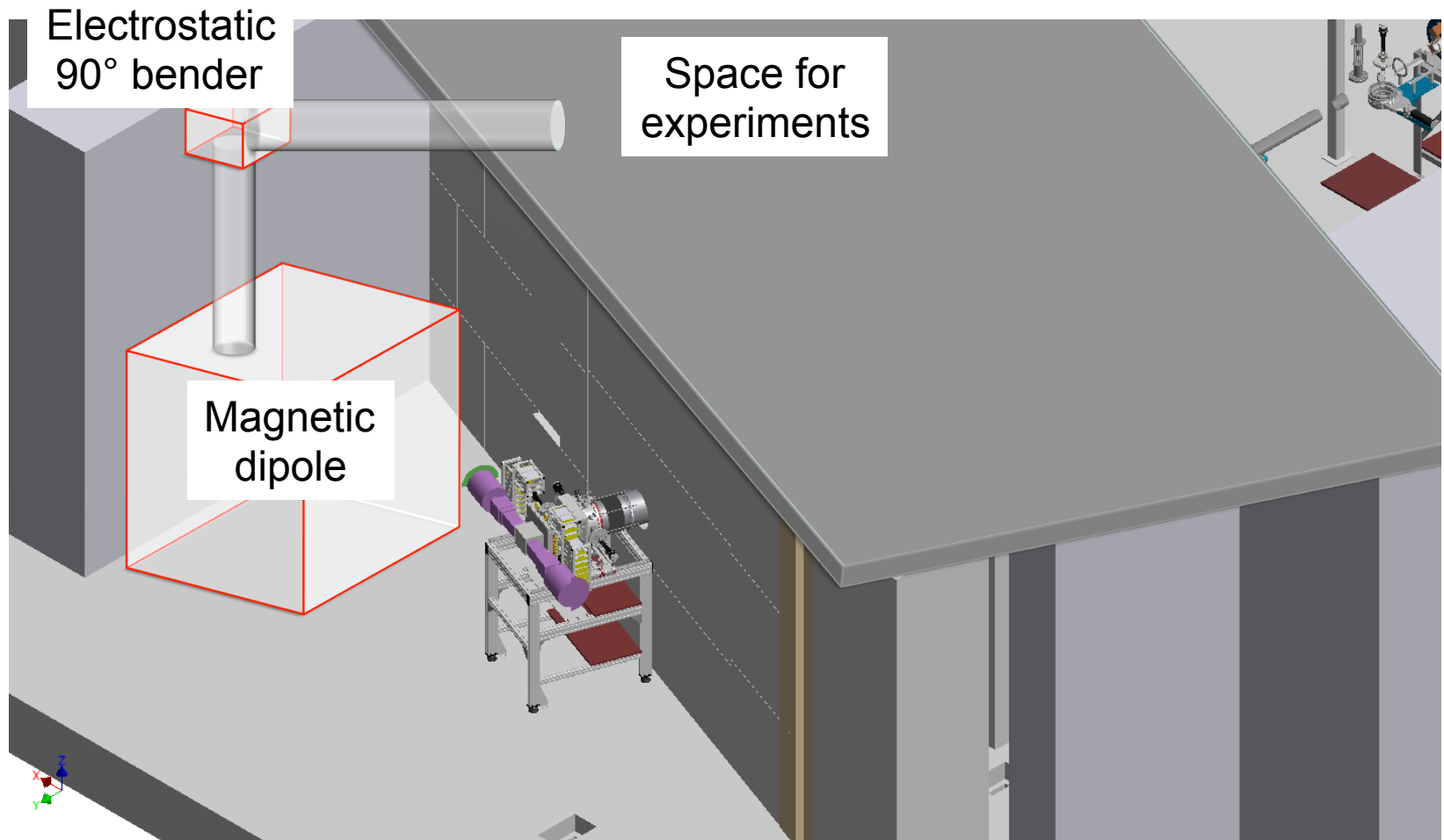
Space requirements



Space requirements



Space requirements



Current Status

Funding:

- Received infrastructure funding from the Academy of Finland, 2016-2018 FIRI
 - 432k€

- MR-TOF-MS for IGISOL funded from Academy of Finland 2014-2016 FIRI
 - 150k€
 - Tommi Eronen
 - Duplicate device to be build for MARA-LEB

Current Status

Equipment

- Tendering for vacuum pumps on-going
- Simulations for the dipole magnet in progress
- Gas cell order by the end of the year
- Ion optics design decided, simulations on-going

People

- MSc student working on the design of the ion guides
- Submitted a number of funding applications for personnel costs

Collaboration



Iain Moore
Philippos Papadakis
Jari Partanen
Ilkka Pohjalainen
Sami Rinta-Antila
Jan Sarén
Juha Uusitalo



Piet Van Duppen
Rafael Ferrer
Yuri Kudryavtsev
Alexandra Zadvornaya

